SANDIA REPORT
SAND2022-11344
Printed August 2022

Sandia National Laboratories

A Summary of Validation Studies for the Integrated TIGER Series Performed on ACORN Plus-up 218468/99

Rowdy Davis (01341, UNM)
Ronald P. Kensek (01341)
Christopher M. Perfetti (UNM)
Aaron Olson (01341)

Prepared by
Sandia National Laboratories
Albuquerque, New Mexico
87185 and Livermore,
California 94550

Issued by Sandia National Laboratories, operated for the United States Department of Energy by National Technology & Engineering Solutions of Sandia, LLC.

Available to DOE and DOE contractors from
U.S. Department of Energy
Office of Scientific and Technical Information
P.O. Box 62
Oak Ridge, TN 37831

Telephone: (865) 576-8401
Facsimile: (865) 576-5728
E-Mail: reports@osti.gov
Online ordering: http://www.osti.gov/scitech

Available to the public from
U.S. Department of Commerce
National Technical Information Service
5301 Shawnee Rd
Alexandria, VA 22312

Telephone: (800) 553-6847
Facsimile: (703) 605-6900
E-Mail: orders@ntis.gov
Online order: https://classic.ntis.gov/help/order-methods/

ABSTRACT

The Integrated TIGER Series (ITS) transport code is a valuable tool for photon-electron transport. A seven-problem validation suite exists to make sure that the ITS transport code works as intended. It is important to ensure that data from benchmark problems is correctly compared to simulated data. Additionally, the validation suite did not previously make use of a consistent quantitative metric for comparing experimental and simulated datasets. To this end, the goal of this long-term project was to expand the validation suite both in problem type and in the quality of the error assessment. To accomplish that, the seven validation problems in the suite were examined for potential drawbacks. When a drawback was identified, the problems were ranked based on severity of the drawback and approachability of a solution. We determined that meaningful improvements could be made to the validation suite by improving the analysis for the Lockwood Albedo problem and by introducing the Ross dataset as an eighth problem to the suite. The Lockwood error analysis has been completed and will be integrated in the future. The Ross data is unfinished, but significant progress has been made towards analysis.

ACKNOWLEDGEMENTS

This would not have been possible without the mentorship of Dr. Aaron Olson (01341), Dr. Ronald P. Kensek (01341), or Dr. Christopher Perfetti (University of New Mexico, Main Campus). A special thank you goes to Dr. Jacquilyn Weeks of Word Tree Consulting for her expert analysis and revisions of key technical pieces, and Dr. Daryl Lee of COSMIAC at UNM for his mentorship in coding methodology.

Supported by the Laboratory Directed Research and Development program at Sandia National Laboratories, a multimission laboratory managed and operated by National Technology and Engineering Solutions of Sandia LLC, a wholly owned subsidiary of Honeywell International Inc. for the U.S. Department of Energy's National Nuclear Security Administration under contract DE-NA0003525.

CONTENTS

LIST OF FIGURES

This page left blank

ACRONYMS AND DEFINITIONS

Abbreviation	Definition
ACORN	Accelerated Collaborative Research Nucleus
ANS	American Nuclear Society
CEE	Common Engineering Environment
ITS	Integrated TIGER Series (Coupled Photon-Electron Transport Code)
LDRD	Laboratory Directed Research and Development
M&C	Mathematics and Computation – a professional conference hosted by the ANS
SEERI	Science of Extreme Environments Research and Innovation
UNM	University of New Mexico
UQ	Uncertainty Quantification
XS	Cross Section

1. INTRODUCTION

This report is based on the work performed in the first two years (FY20-FY21) of the ACORN plus-up to the Next-Gen Monte Carlo LDRD, (Project Number 218468):

Work in Year 1 will involve a UNM student working with Perfetti [Dr. Christopher Perfetti of the University of New Mexico] and SNL staff to expand the ITS validation suite by modeling experiments during the school year as well as a summer internship at SNL. In addition to the immediate benefit of a stronger validation suite for SNL's radiation transport code ITS, this work will familiarize the student with photon/electron transport using ITS as well as add to the library of simulations needed for future uncertainty analysis and data calibration efforts.

These Year 1 goals were extended into a second year during which we were invited to establish a stronger foundation for the further expansion of ITS. A student worked as a contractor through UNM on the project during the academic year and was hired as a summer intern in 2020 and 2021 (strengthening the hiring pipeline) as proposed. Several experiments were modeled (see Section 2 of this report), and two peer-reviewed conference papers were written on those efforts and results. The student gave numerous presentations based on the work including two conference presentations, a talk at the ANS Trinity Chapter in Albuquerque, and several presentations at UNM and SNL . In addition to the immediate benefit of strengthening the ITS validation suite, we have also helped build a library for UQ/data calibration efforts as proposed.

2. TECHNICAL HIGHLIGHTS

This section briefly covers the technical work reported in two professional papers [1-2] and the preliminary work for the Ross Electron Transmission data (called "Ross data") [3] which sets the foundation for future technical analysis. More about the Ross data can also be found in Section 4 – Legacy.

2.1. Preliminary Evaluation of the ITS Validation Suite

In the paper [1] related to this section, the primary goal was to identify weaknesses in the validation suite that could be improved. A surface-level analysis was conducted on the (then) validation suite's seven test problems, which covered different types of target materials, particle energies, and angles of particle incidence. We assessed that uncertainty quantification (UQ) comparisons were primarily qualitative through "viewgraph norms" and that developing a more quantitative approach could strengthen the suite. Therefore, we determined that our best course of action for the initial expansion of the validation suite was to add more rigorous UQ in the Lockwood Electron Albedo problem [2] and eventually increase the number of cases simulated.

2.2. Revisiting the Lockwood Electron Albedo for ITS

The Lockwood Electron Albedo [2, Appendix A] problem was determined to be a strong initial candidate for expansion of the suite. The problem has simple, one-dimensional geometry, it contained over 200 individual measurements with a wide range of angles, a range of elements that varied significantly in Z (atomic number) and a decent band of energies. The Lockwood Electron Albedo provided a great starting point to learn about the intricacies of ITS. Given the wide range of experimental measurements, the problem offered a clear and simple process for varying simple parameters. Since uncertainty quantification was available for this problem set, it was determined that the suite could expand in a meaningful way with the largest initial impact due to the number of materials, angles, and energies present. In the analysis, substep size, problem thickness (defined as default in the paper versus what Lockwood uses), glancing effects, energy cutoffs and the use – or lack thereof – of electron trapping were examined. The aim was to understand how varying these problem parameters contributed to error and, of the two error metrics analyzed, (see Section 2 of [2]), how they changed as a function of the changes to the problem. It was observed that 90% of the comparisons were within ±5% relative error which is acceptable to most stakeholders of ITS. However, only 75% of these measurements were within two standard deviations of the combined aleatoric uncertainties, which suggests that there is some systematic bias in the results, although the error itself does not assist in identifying whether the bias is in the measurements, the simulations, or the UQ in either/both. These findings have demonstrated a methodology that is useful going forward and which will accelerate future investigations that will find additional evidence for assessing the predictive simulation capability of ITS.

2.3. A Brief Look at the Ross Data

We then established a strong foundation for further technical analysis using the Ross data [3] by performing ITS simulations of the angular distribution of transmitted electrons to compare with the Ross measurements, by writing scripts to expedite the analysis of the experimental and simulated data, and by creating plots for qualitative comparisons. Prior to this analysis, there was no ITS analysis for the Ross data. Currently, no quantitative error has been calculated and no parameter studies (e.g., angular offset, error in distance, some thickness variance, etc.) have been conducted, but we have created the framework for future work.

3. PROJECT METRICS

3.1. Mentoring

The student was under the primary mentorship of Dr. Ronald P. Kensek (01341) and Dr. Aaron Olson (01341). Dr. Olson taught skills in time management and assisted in furthering the student's technical writing skills, as did Dr. Jacquilyn Weeks. The student published a Senior Thesis (Appendix A), a student conference paper [1], and a professional conference paper [2]. The team was mentored by Dr. Jacquilyn Weeks in the creation of a more effective presentation and technical poster and gave a total of three presentations at external, professional venues. Dr. Kensek explained complex transport concepts in such a way that the student (who was new to the field) could understand them and utilize them. He also taught the student how to write ITS input decks and find the relevant results inside the output files such that his instruction was key to the student's progress in the projects discussed.

3.2. Technical Skills

Evaluating and improving ITS required a vast amount of data creation and data analysis. Doing this by hand is tedious and not worth the time and effort required, especially since a lot of runs use data that may be different from the data used in a previous run. To that end, the student needed to learn how to write Bash scripts, familiarize with the Linux terminal and its respective commands, and strengthen Python programming skills. Bash scripts were written primarily to sift through the Lockwood data to identify flags that would be used to find the electron albedo values at certain angles and energies, and then convert them into .csv files to make it easier to pull the data into Python as organized arrays. Bash scripts were also used to initiate a mass set of runs for ITS at once. Instead of manually typing Linux commands including the executable, the input file, and the output file, the student wrote a Bash script and called the Bash script once per run. Familiarizing with the Linux terminal and its relevant commands allowed the student to organize data storage sites depending on which data sets were being run, which experiment was being studied, and how the particular data was organized for each experiment. Learning how to send and pull files off a server was critical as ITS could not run locally and had to run server-side. Python was instrumental in creating ITS input files and mass data analysis. When performing work on both the Lockwood and Ross problems, one script was used to generate the inputs based on energy, angle, and material (for Lockwood) and energy, thickness, angle, and material (for Ross). For data processing, with respect to Lockwood, .csv files were read into Python, relevant operations were done to the data, and then the respective plots were generated. For the Ross data, the same was partially true, except that between analyzing Lockwood's and Ross's experiments (about a year's time) the student was able to learn how to sift through data in Python and not use an extra script to pull it together, and then use that same script to process the data and output the plots. This improvement in skill and understanding in Python helped streamline development on the project.

4. LEGACY

All codes that have been written for the entirety of this project are accessible on the CEE servers under the "radeff" directory. Those interested in accessing them should reach out to Dr. Ronald P. Kensek (01341) or Dr. Aaron J. Olson (01341). All currently published papers pertaining to the technical work can be found either as a reference in this report, in the appendix below, or as references in the papers written (see Reference 1 and 2). All presentations and posters on this topic can be found in the Sandia technical library, locatable by searching for Rowdy Davis.

At present, the comparison to the Ross data is a work in progress. To date, results of new work with the Ross data have not been documented beyond the brief description here. Comparison to the Ross experiment is not currently part of the ITS validation suite, but such future work is along with similar uncertainty quantification that was done with the Lockwood data. A code exists for both creating input decks, running the input decks through ITS, and then processing the results. Unlike Lockwood's data, the Ross data is run two times for a complete analysis. It is recommended, for the way the codes are written presently, to run the ITS simulation for 13 MeV and 20 MeV separately unless one decides to modify the XS data decks. The analysis code can be run once for all data points. These codes will also be available in the "radeff" directory. A text file will be present for each code explaining the code's function, file naming conventions, and any other relevant information necessary to understand the process of data analysis used. The codes may also be broken up into smaller segments for any developer that wishes to utilize certain frameworks present in each code. No uncertainty quantification has been performed for the Ross data.

For the Ross data, graphs like the figure below have been produced, which are akin to those produced by Ross *et al.* [3]. The Ross data has a central point, at 0, and there are positive steps away from 0 and negative steps away from 0, all in centimeters. To re-create Ross's data graphically both with his data and ITS data, the cm distance was converted to an angle by taking the inverse tangent value of the length value divided by either 115.4 (if the material is not Ti) or 118.2 (if the material is Ti). Those values are discussed in the appendix of [3]. Those angles are used in ITS but are all positive and shifted to be consistent with the Ross measurements due to the measured peak versus the experimental setup. The "RossFileGen" Python script does shifting for the user. From there, the data is then processed in Python where the data that tends negative from Ross's dataset is called "N data" and the positive half is called "P data." Once the Ross raw data is in Python along with the ITS output response function, the data is all normalized to the peak, and then plotted on one graph for a particular material, energy, and thickness combination.

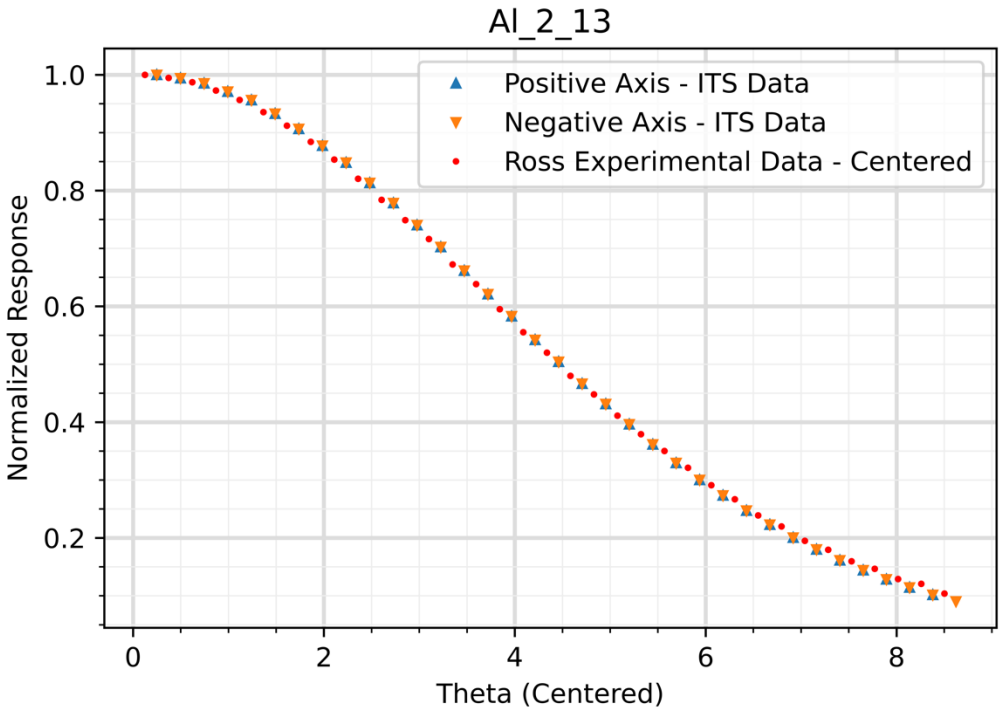

Figure 4-1. Aluminum at 13 MeV, 0.0518519 cm thick

Some discrepancy between the "red dots" and the "orange and blue triangles" is observed in this plot, though that discrepancy has not yet been quantified. The next step is to quantify the discrepancy and verify that the correct bins are being used.

REFERENCES

[1] Davis, Rowdy; Perfetti, Christopher; Kensek, Ronald P.; Olson, Aaron J. and Franke, Brain C. *Expansion of the Monte Carlo Integrated Tiger Series Validation Suite.*. United States: N.p., SAND2020-2645C. 2020. Web.

[2] Davis, Rowdy; Kensek, Ronald P.; Olson, Aaron J. and Perfetti, Christopher. *Revisiting the Lockwood Albedo Measurements for Validation of the Integrated Tiger Series Electron-Photon Transport Code.* United States: N.p., SAND2021-3813C. 2021. Web.

[3] C. K. Ross, et al., *Measurement of multiple scattering of 13 and 20 MeV electrons by thin foils*, Med. Phys. 35 (9), p. 4121, 2008.

[4] Lockwood, G.J.; Ruggles, L. E.; Miller, G. H.; and Halbleib, J. A.; *Electron Energy and Charge Albedos Calorimetric Measurement vs Monte Carlo Theory*, Tech. Rep. SAND80-1968, Sandia National Laboratories. 1981.

[5] Franke, Brian C., et al., *ITS Version 6: The Integrated TIGER Series of Coupled Electron/Photon Monte Carlo Transport codes, Revision 5*, SAND2008-3331, Sandia National Laboratories, PO Box 5800, Albuquerque, NM. 87185, September 2013.

APPENDIX A. SENIOR THESIS

A Senior Thesis:

Expansion of the Monte Carlo Integrated Tiger Series Validation Suite

Submitted for Departmental Honors

on

May 15th, 2020

Rowdy Davis, University of New Mexico, Department of Nuclear Engineering

Dr. Christopher Perfetti, University of New Mexico, Department of Nuclear Engineering

Dr. Ronald P. Kensek, Sandia National Laboratories

Dr. Aaron Olson, Sandia National Laboratories

Dr. Brian Franke, Sandia National Laboratories

Abstract

The ITS (Integrated Tiger Series) code is a valuable modeling and simulation tool for predicting radiation damage in photon and electron radiation environments. In order to improve the current ITS (Integrated Tiger Series) validation suite, the code was looked to be improved upon in three ways: adding tests from Lockwood's 1981 experimental data, make quantifiable assessments on the simulation versus measurements, and script the creation and execution of the test data to automatically compare with future versions of the code. The preliminary results from these simulations show agreement to within two percent relative error at high energies, for all angles, for all but the lower atomic-number materials. At the lower energies, the disagreement is larger for the larger angles. While there were variations for different materials, the electron source energies ranged from about 0.3 MeV to 1 MeV, and the source directions ranged from about zero to 75^{o} with 15-degree increments. The eight materials were chosen to cover a practical range of the periodic table.

Introduction

The Integrated Tiger Series (ITS) program is a Monte Carlo code for simulating Coupled Electron-Photon Transport [1,2]. It is used normally to assess the radiation hardness of complex systems, such as components for satellites in space. The ITS code is currently maintained by Sandia National Laboratories. This work's goal is to discuss the status of the code and decided course of action for areas of improvement and validation / verification of the ITS Validation Suite. This validation suite is used to assess the accuracy of ITS simulations, and at present consists of seven examples with three methods of transport per example. The three methods of transport used are the condensed-history method, the hybrid multigroup / continuous energy method, and the single scattering, analogy method. Significant gaps in validation coverage exist for photons and electrons in many areas such as source energy, source direction, target material, and quantity of interest – to address these gaps, additional experimental data were sought out, simulated, and will later be added to the validation suite to create a more robust test suite.

The seven cases are described in the table below, which includes assessments and observations regarding each experiment's strengths and limitations.

Representative Tests in the ITS Validation Suite [1]

TABLE I. Current Coverage by the ITS Validation Suite

Experiment	Energy	Material	Assessments and Observations
Lockwood Electron Albedo [3]	0.032 – 1 MeV	Uranium	Error increases for more glancing angles. Analog issues above 256 keV.
Hanson Electron Angular Scattering [4]	15.7 MeV	Gold	Could the parameter studies be cast in terms of convergence studies? Could a sub-step size be added for condensed history? Analog fails to capture peak.
Tabata Charge Deposition [5]	14.9 MeV	Beryllium	Analog misses depth location of peak energy depositions, and slight distortion of shape.
McLaughlin Energy Deposition [6]	3 MeV	Aluminum	Analog misses depth location of peak and shape of distribution.
McLaughlin Energy Deposition [6]	100 keV	Polystyrene	All methods miss the measured tail. Cannot properly assess how well any method captures the peak.
Sanford Radial Dose Profile from Bremsstrahlung [7]	750 keV	Carbon	Difficult to assess how far off the last measurement is. Analog has issues.

Dolan Electron Emission from Photons [8]	50 keV endpoint Bremsstrahlung spectrum	Tantalum	Disagreement between all models and experiments under 20 keV for all methods.

These seven experiments ultimately show disagreement with analog data, with no quantitative assessment in the reporting of comparisons, or their accuracies. The current understanding of the benchmark data solely resides in graphs that point out trends such as miscalculations of the depth location of energy deposition peaks and failure to compute the expected shape of the overall energy deposition [1]. When viewing the plots in the Franke and Kensek paper, there is no quantification of numerical error for the data, some plots lack error bars, and those that do have error bars on the plots don't effectively demonstrate what those confidence intervals are (i.e. one sigma, three sigma, or some other decided interval). The goal of any validation program should include an output of quantitative comparisons.

Due to time constraints, it was decided to simply focus on one of the test cases: the Lockwood Electron Albedo experiment [3]. Franke and Kensek [1] mention the Lockwood experiment, but do not incorporate these tests in the automated test suite. There is also no mention of any quantitative error on the accuracy of the current test suite for any data – let alone the Lockwood data. The Lockwood data examined by Franke and Kensek only concerns Uranium. This paper explores the expansion of the Lockwood experiment by simulation of other materials to better cover the range of the periodic table by utilizing the condensed-history method of transport. The materials explored are Uranium Dioxide, Beryllium, Carbon, Tantalum, Titanium, Molybdenum, and Aluminum.

Theory

Current ITS Transport Methods

Currently, the ITS validation suite includes seven physical benchmark examples, and utilizes three forms of transport in each of the seven examples. The three transport methods in ITS are the condensed-history method, a hybrid multigroup/continuous-energy method, and a single-scattering method [1]. All three methods use similar cross-sectional data. For bremsstrahlung production, the condensed history uses angular distributions from the Bethe-Heitler theory, and the multigroup/continuous energy use a simpler model, which is similar to that in MCNP. When examining the relaxation cascades, they are similar for both the multigroup and condensed methods, however there are slight differences between the two. The single-scatter method (which can also be referred to as the analog method) uses a complete set of subshell data for the relaxation cascades.

All three methods in ITS have a different energy-loss model and vary in their treatment of both large and small energy-loss interactions. For the condensed history method, it works off of a pre-computed energy-loss, as well as a pre-computed set of angular-scattering distributions. Electron tracking is separated into sub steps, with collisional energy loss sampling at the start of each step. Angular scattering is computed over a sub step centered in the middle of a step with the use of Goudsmit-Saunderson expansion. Angular deflection in part of inelastic-scattering is accounted for by adjusting the elastic-scattering distribution with the assistance of a (Z+1)/Z correlation [9]. Energy loss is sampled over a step from the Blunck-Leisegang distribution with a

Seltzer [10] distribution correction. The Jordan-Mack algorithm is used for boundary crossings. Bremsstrahlung photon production, knock-on electron production, and ionization events are sampled for each sub step.

The hybrid multigroup model estimates adjoint fluxes by transposing the group-to-group matrix already present within the code. What this allows for in this particular transport method is calculating a very specific quantity of interest (an example would be dose in one volume or point) and gets the answers for a variety of sources of different energies, spectra, or directions. This is accomplished by using the inner product as a multidimensional integral over phase space, where the operator for this would be the forward Monte Carlo transport code [11]. This model is coupled with the CEPXS code, which takes cross sectional data and integrates it over each particular group. Sixty-three scattering angles are used in this process.

The single-scattering transport is based on the LLNL EDL. The EDL data is represented in tabulation with mostly prescribed interpolation schemes. The EDL (electron data library) deals with four types of cross sections: ionization, excitation, elastic scatter, and bremsstrahlung. These are all tabulated as a function of the incident energy of the electron, with different grids used for each set of energy data. The single-scatter algorithm for elastic and inelastic electrons makes electron transport computationally expensive, but it can be reasonably applied to low-energy problems. The relaxation model that is present in this is far more detailed than anything in ITS presently and is still a rather recent implementation to the code that requires further testing.

Lockwood Electron Albedo

The albedo test deals with the Lockwood's measurements of the electron number albedo. It is known that in the condensed-history algorithm that the results are underestimated due to straight sub step mechanics. The error of the model in ITS shows that error increases for more glancing angles. While the primary form of the experiment from Lockwood is dealt with through charge depositions, when the material thickness is greater than the range of any impinging electrons on the minimum z surface, Lockwood notes that when bremsstrahlung losses are small, the complement of the deposited energy yields "indirect yet more reliable values of saturated integral electron energy albedos." [3]. It is important to note though that this is more accurate for higher Z materials, and more so, that the uncertainties are larger for lower atomic-number materials, especially at lower energies.

Methodology

Data Acquisition

In Lockwood's paper [3], he mentions that his method is more accurate for higher Z materials, and the RPSD paper from Franke and Kensek [1] look at Uranium in their ITS run to make their comparisons. The following test cases were decided upon, based on the measured electron number albedos available from Lockwood's report [3].

ITS Simulations

TABLE II. ITS Simulation Test Cases

Target Material	**Source Energies (MeV)**	**Source Angles**	**Total Cases for Material**
Beryllium	0.109, 0.314, 0.521, 1.033	1, 16, 31, 46, 61, 76, 83.5	28
Aluminum	0.032, 0.058, 0.084, 0.109, 0.314, 0.521, 1.033	0, 15, 30, 45, 60, 75	42
Carbon	0.025, 0.05, 0.075, 0.1, 0.3, 0.5, 1	0, 15, 30, 45, 60, 75, 82.5	49
Molybdenum	0.109, 0.314, 0.521, 1.033	0, 15, 30, 45, 60, 75	24
Titanium	0.109, 0.314, 0.521, 1.033	0, 15, 30, 45, 60, 75	24
Tantalum	0.032, 0.058, 0.109, 0.314, 0.521, 1.033	0, 15, 30, 45, 60, 75	36
Uranium	0.032, 0.058, 0.084, 0.109, 0.314, 0.521, 1.033	0, 15, 30, 45, 60, 75	42
Uranium Dioxide	0.1, 0.3, 0.5, 1	0, 15, 30, 45, 60, 75	24

For each respective material, each source energy is tested. For each source energy, each source angle is tested. The angles are the number of degrees off from a normal incidence. This is how the total number of cases per material were found, and how each test input file for ITS was then made. In order to automate this process, a python script was created to generate these files given certain input parameters. These input files were written in such a way that they could be fed into ITS with the assistance of a bash script, which allowed for an ease of running ITS given the multitude of input files.

From there, another script was written which went through the ITS output files and collected the relevant albedos at each energy and angle, for each material. The output data was then gathered into a file for each material.

Scripting

Due to the large amounts of experiments to run and then process, scripting was an unspoken requirement. To this end, Python and Shell were used in order to write and then execute the scripts. In generating the input decks, Python was used to execute a combinatorial process to combine the information in table 1 effectively and accurately. List comprehension was used to take a particular material, and parse through every angle, for each energy. This led to “n” number of files in the “Total Cases for Material” column of table 1, which then created a sum of 269 different input decks. The cross-sectional data for these input decks was not scripted, as only 8 files were required. In the future, if multiple sets of cross-sectional data may be required (which was not the case in this instance), a very similar combinatorial process could be used via Python (or another language of choice) with the assistance of list comprehension. In order to run these 269 cases, a Shell file was created with the execute commands for each of these cases. This was rather long winded, and a script to make a script could be created, but that was not done in this instance. This shell file ran the 269 1-D ITS commands and placed them in the same directory. Following that, all the materials were separated into different directories, based on their material type. From there, another script was written to parse through each of the result files and create a .xlsx file with their respective albedo, their associated error, and their identifying

features (angle, energy, and material). This .xlsx file was used to then initiate data processing. While it may have been possible to then automate data processing, and tie it in with data retrieval, it was not done in this instance, but may be useful in the future.

Data Processing

Following the data gathering from the simulations ran in ITS, the data from Lockwood's report was gathered into the one excel file, as he had relevant number albedos to make a comparison to for this set of simulation data. From there, relative error was calculated to demonstrate how near or far the simulation data was from the actual data of Lockwood's experiment. The following equation was used for that:

$$Rel\ Err = ABS(\frac{A_s - A_l}{A_l}) \qquad Eq.\ 1$$

where A_s and A_l represent the simulation albedo value and the Lockwood albedo value, respectively.

When looking at error for each data set, it was important to quantify the error for each data point, as each respective angle and energy combination had some error associated with it, both from the simulation, as well as from Lockwood's data. When examining the error from the simulation, the only error looked at in this case was that of the Monte Carlo runs, which were given in a percent of the value. In this particular instance, it was either 0 or 1, which was a function of how many batches and histories per batch were ran. As the highest uncertainty was expected in the smallest Z material, the runs were decided such that this number would be minimalized while still allowing a reasonable amount of run time. The particular uncertainties from the simulation can be viewed in the appendix for each material, energy, and angle. In regard to the Lockwood errors, it is first important to note that he did not publish his uncertainties for carbon and gave a range of values for UO_2 which were very different from his data given for other materials. Secondly, the albedos that he does show error for are merely at 0 (or 1 degree in Beryllium's case) and 60 degrees (or 61 for Be), and not for any other angle. He states that they hold for all energies though, as an approximation. Due to that inconvenience, the goal then became to use his equation from the 1975 study to recreate the error uncertainty calculations [12]:

$$100\ k_i(1-f)^{-1}\left[1+\left(\frac{k_d}{k_i}\right)^2 f^2\right]^{\frac{1}{2}} \qquad Eq.\ 2$$

Lockwood [3, 12, 13] did not publish his values for k_i or k_d (uncertainties of measured currents involved in his determination of the number albedo), which makes recreating his attempt at using this exact equation for any form of error analysis rather difficult. A modified equation is then used which Lockwood states is a close approximation (but how "close" is never stated). With that, the Lockwood error, or E_l, can be calculated.

$$E_l = C * \frac{1}{1-f} \qquad Eq.\ 3$$

Where C is the proportionality constant, which changes (or can change) for each material, and 1-f is the Lockwood number albedo. In order to figure out what E_l and C are simultaneously, the equation is solved without C, where for ~ 1 MeV, at 0 and 60 degrees, E_l is known. C is then iterated on to come to a value where E_l matches the Lockwood percent error at the two aforementioned data points. It is then assumed that this value of C holds for the remaining points in the same material for all energies and angles. This of course may introduce some error as well. In regard to the previously mentioned simulation error, it is a function of the percent error from the Monte Carlo calculation, and the number albedo. The process for that is seen below:

$$E_s = \frac{M + 0.5}{100} * A_s \qquad \textit{Eq. 4}$$

where M is the Monte Carlo error (as a percent), and A_s is the simulation albedo. When looking at the case of beryllium, the angles of 1, 16, and 31 degrees are 1, for all energies are reported as 1 percent. For every other material, all angles and energies are reported as 0 percent. Because there is only a single degree of precision, it is possible that these range up to 1.49 for 1 percent, and up to 0.49 for 0 percent, but are simply rounded down. They may also lie anywhere between the reported value and the highest possible value. However, it is believed that due to the number of batches and histories per batch that these uncertainties, especially at higher Z materials, are quite low.

With the albedos from Lockwood and this simulation, as well as respective errors from both, it is then possible to calculate the overall test statistics for this simulation. The reasoning behind this is to quantify the accuracy of the simulation. To do this, the following equation was used:

$$T = \frac{A_s - A_l}{\sqrt{(E_s)^2 + (E_l)^2}} \qquad \textit{Eq. 5}$$

T represents the error relative to the combined statistical error, with a value as close to 0 as possible representing the best of the statistics. Comprehensive tables for each material may be seen in the appendices. This will be discussed further in the results section of this paper.

Results

Beryllium

When investigating the number albedos generated from the simulation, in the higher angles, there is a rather linear trend in the data, which also is rather similar to the Lockwood data. As the angle dips below 46 degrees, the data becomes less linear across the range of energies of interest (0.109 MeV to 1.033 MeV). The error bars on this data represent the error of the Lockwood data, shown against the simulation data to illustrate the “closeness” of the simulation data with regard to the Lockwood data.

FIG. 1. Incident Energy v. Fraction of Electrons Backscattered for Beryllium

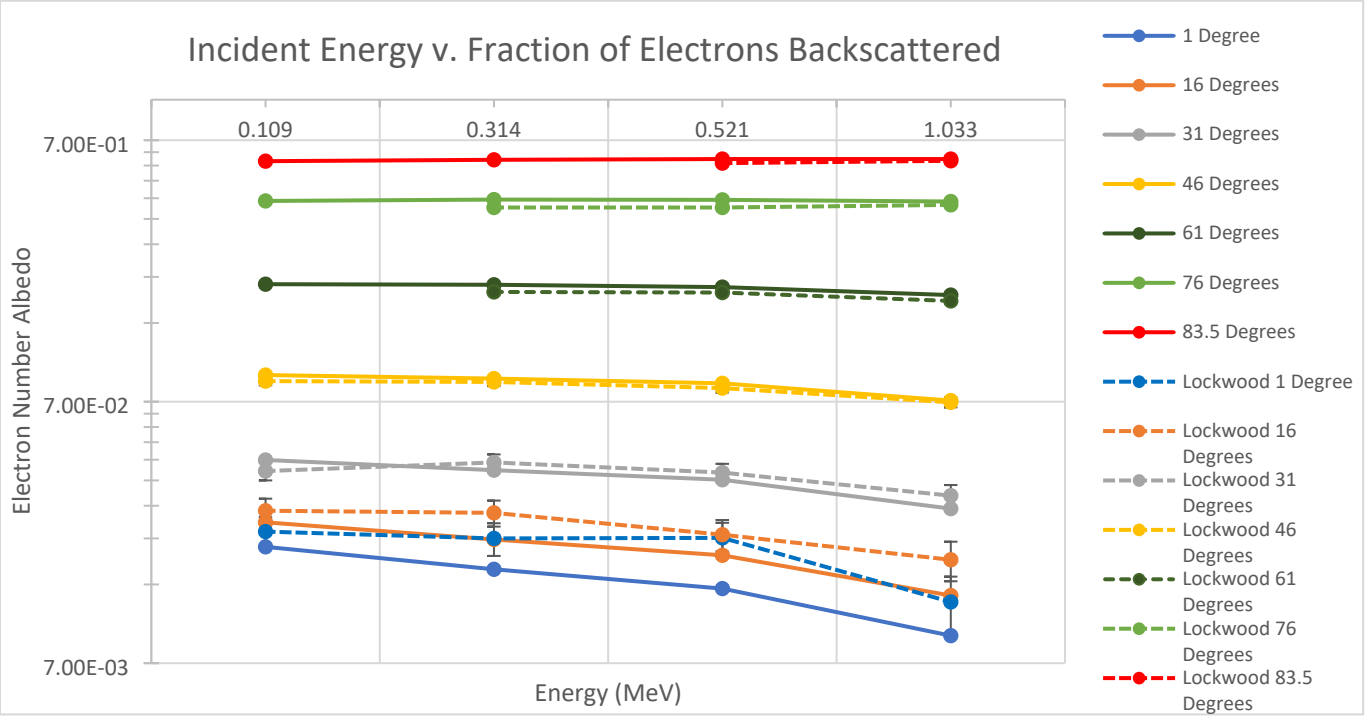

While no error appears to be present for the simulation data, the matter is that it is there, just extremely small for Beryllium's case.

In order to further see how the data generated in the simulation compared to that of Lockwood's, relative error was looked at to make that comparison. Just as error was larger for the Lockwood data at higher angles compared to his lower angles, this holds true for the relative error as well. A table of all relative error data can be seen in the appendices.

FIG 2. Relative Error for Beryllium

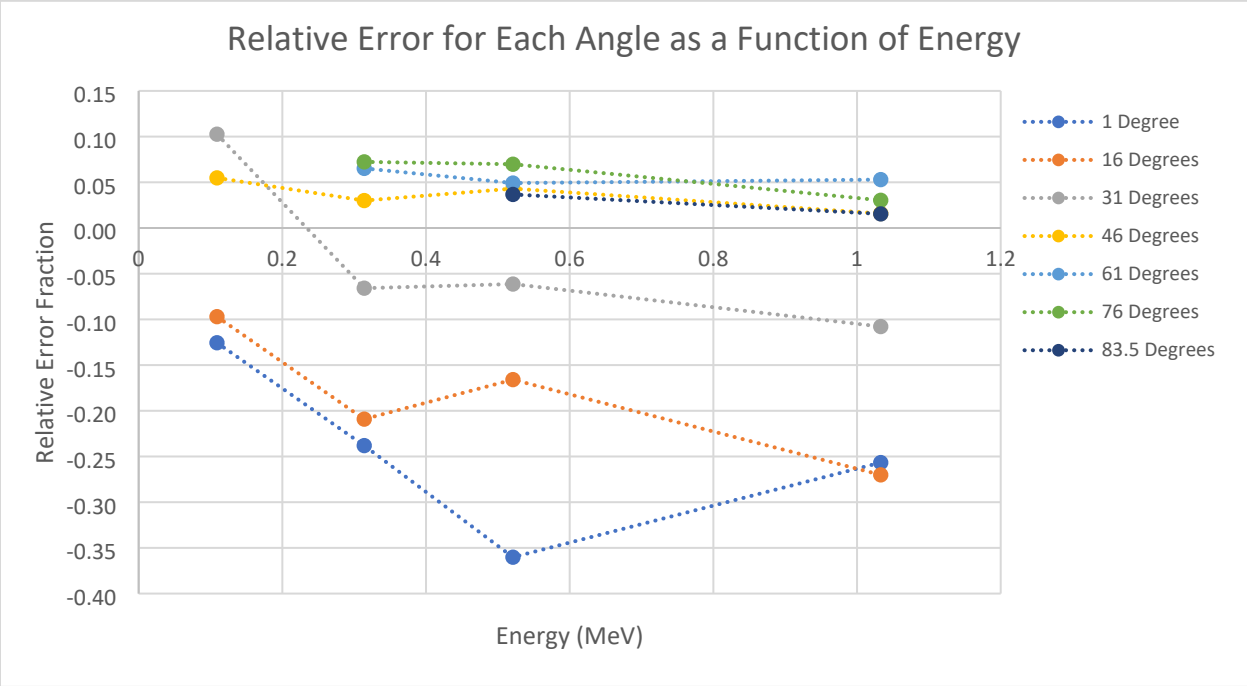

While this shows the relative accuracy between each point, in and of themselves, the need to show a quantitative analysis of how accurate the data may be leads to an overall test statistic. These test statistics are the relationship between each of the points, akin to relative error, but also take into account the error for each of those albedos, when making the relationship comparison. When viewing this data, the overall error is smaller at lower angles, and higher energies. As the angle increases, the error does as well. Error decreases for all angles as energy increases. There are also no values from the Lockwood data in terms of experimental error for the higher angles.

FIG. 3. Error relative to the combined statistical error for Beryllium

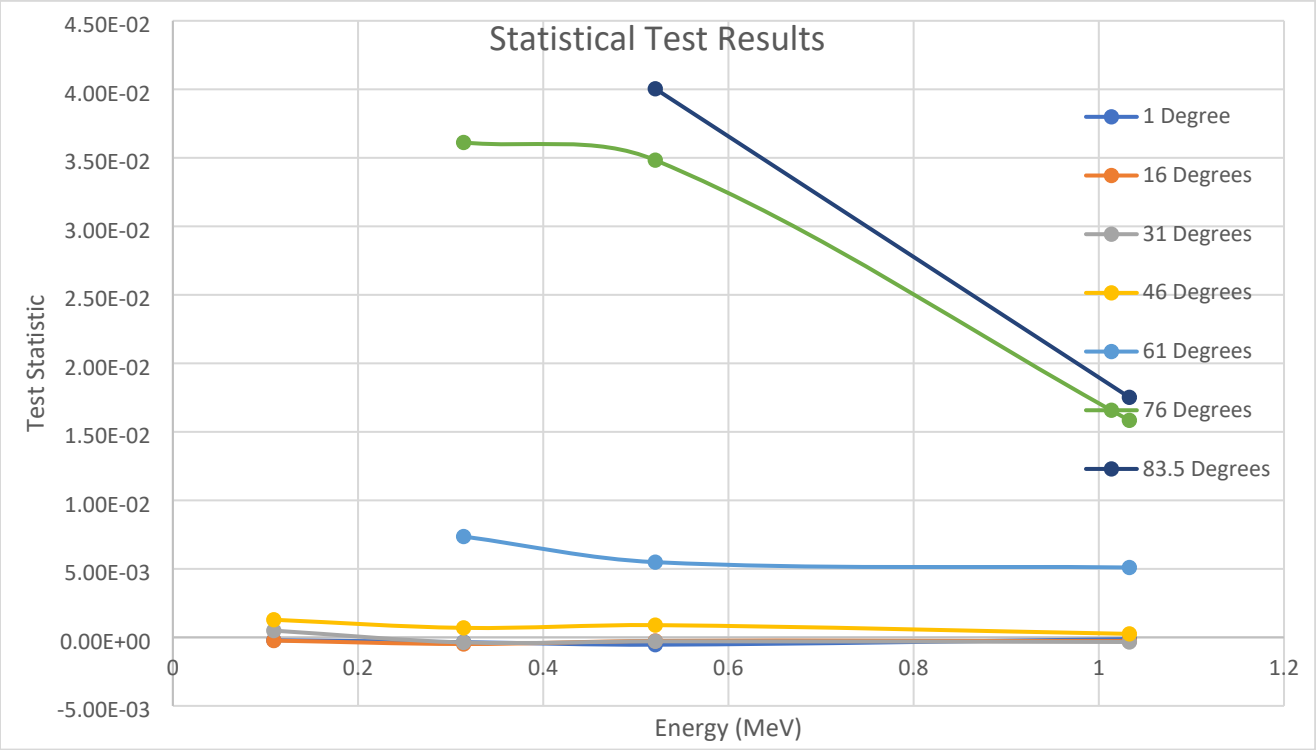

Aluminum

Aluminum shows good agreement in the lower energy levels at 0 degrees, but as the angles increase, it appears that the experimental data and the Lockwood data start to deviate as the energy level increases at 0.032 MeV. As the energy levels increase, however, the agreement between the Lockwood data and experimental data increase for all angles. The error in the Lockwood data at 0.032 MeV does not align with the experimental data from ITS, which may indicate that either ITS does not simulate these lower energies well.

FIG. 4. Incident Energy v. Fraction of Electrons Backscattered for Aluminum

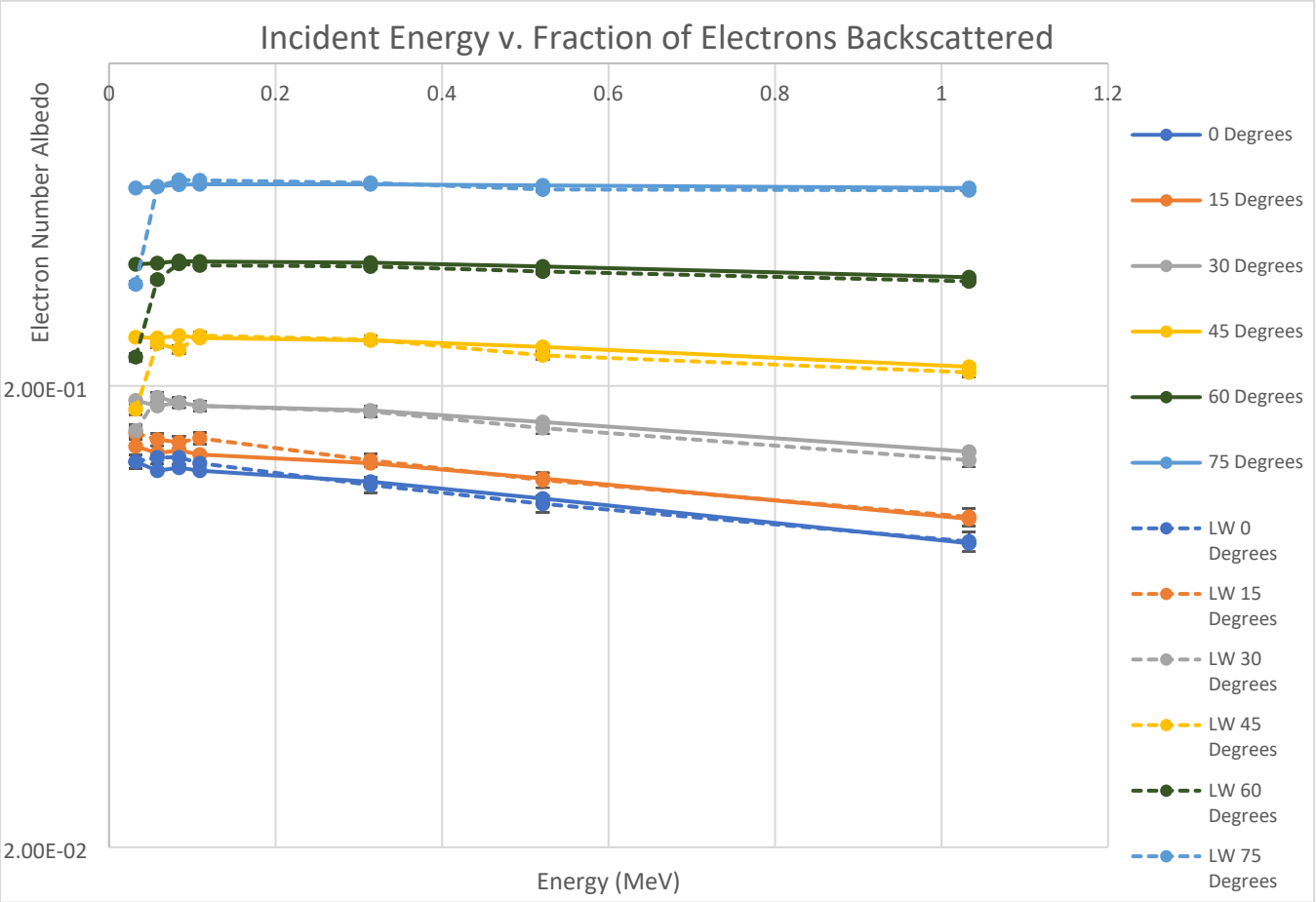

This trend in the data above is expressed even more so when looking at the relative error. This point at 0 degrees and 0.032 MeV can be seen in the appendix for Beryllium Relative Error. Apart from the lower energies and angles, the relative error in the data set is rather low, showing good agreement between the simulation data and Lockwood's data.

FIG. 5. Relative Error for Aluminum

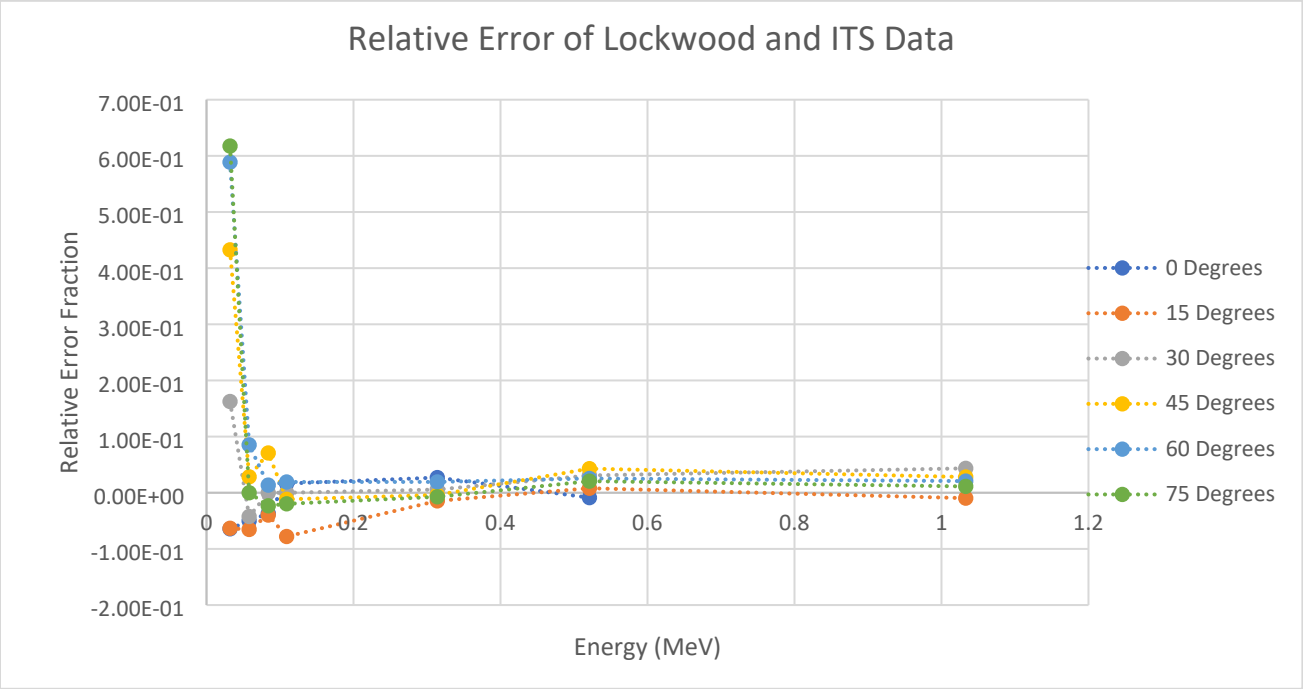

The above trend is also seen when examining the overall test statistics for Aluminums case. The highest values (demonstrating the least amount of agreement in the data comparisons) occur at the higher angles and lower energies. As the energies increase though, agreement becomes very strong.

FIG. 6. Error relative to the combined statistical error for Aluminum

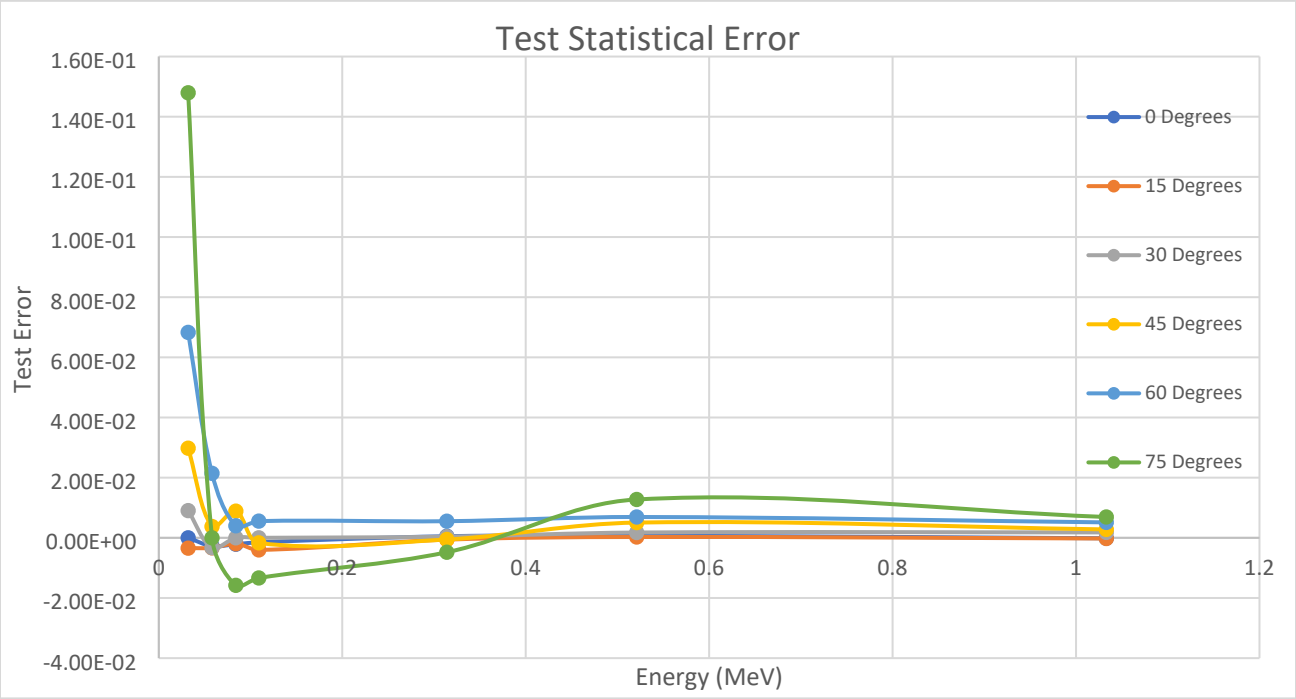

Carbon

When looking at the relationships between Lockwood's albedo data and the ITS simulation albedo data, it appears that there is good agreement between all energies in the lower angles., however this is not necessarily the case. The relative error plot will show that there is in fact the largest values of relative error present at the lower energies. As the energy levels increase, the error appears to minimize, however for 0 and 60 degrees, the error increases once more at around 1.033 MeV.

FIG. 7. Incident Energy v. Fraction of Electrons Backscattered for Carbon

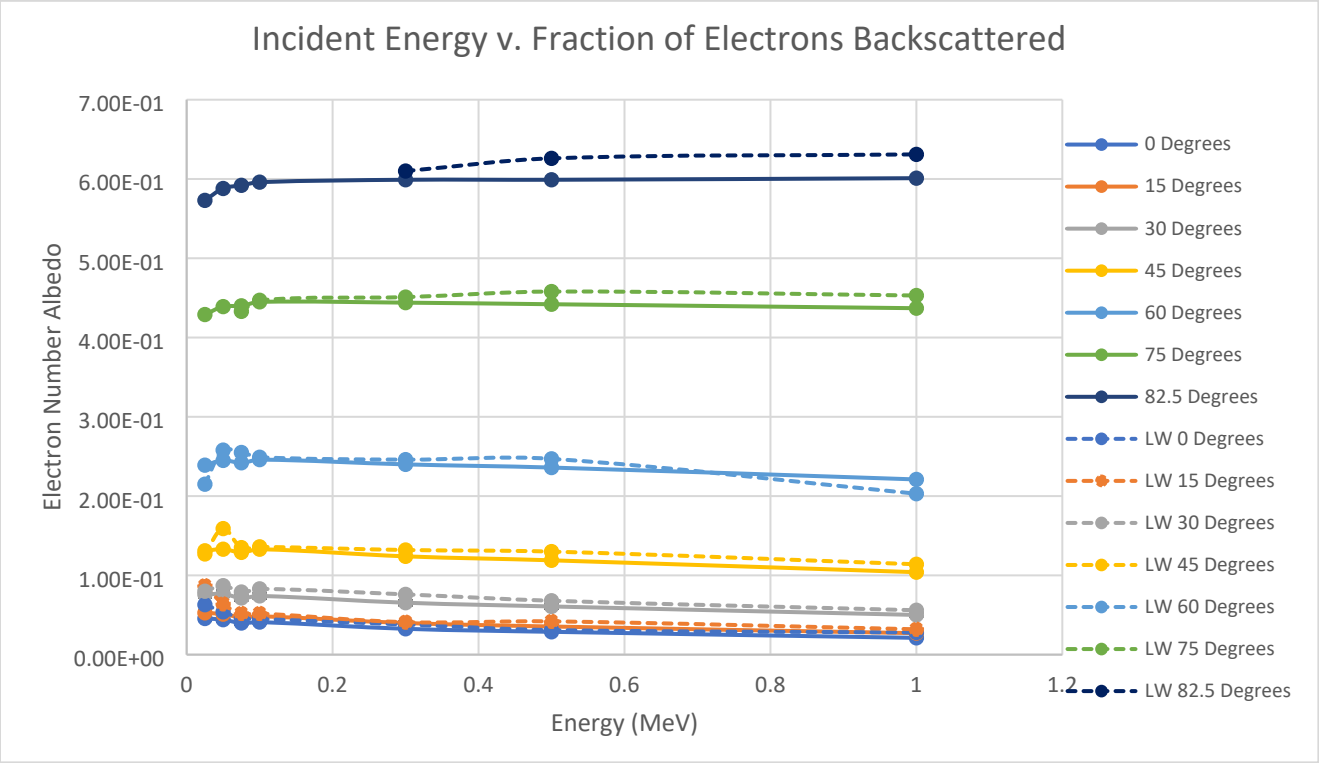

Error bars do exist for this figure, at least for the Monte Carlo errors, however due to their relatively small size, they are minimal and difficult to see, if at all. Lockwood did not provide any quantitative assessment of error for his experiments, so there is nothing to go on in regard to his data. As mentioned previously, figure 8 shows little convergence, which is primarily illustrated by the lack of a trend throughout the entirety of the relative error results. 0 and 60 degrees have initial large relative error, it decreases and then increases once again. This is seen in 15 degrees and slightly in 45 degrees as well.

FIG. 8. Relative Error for Carbon

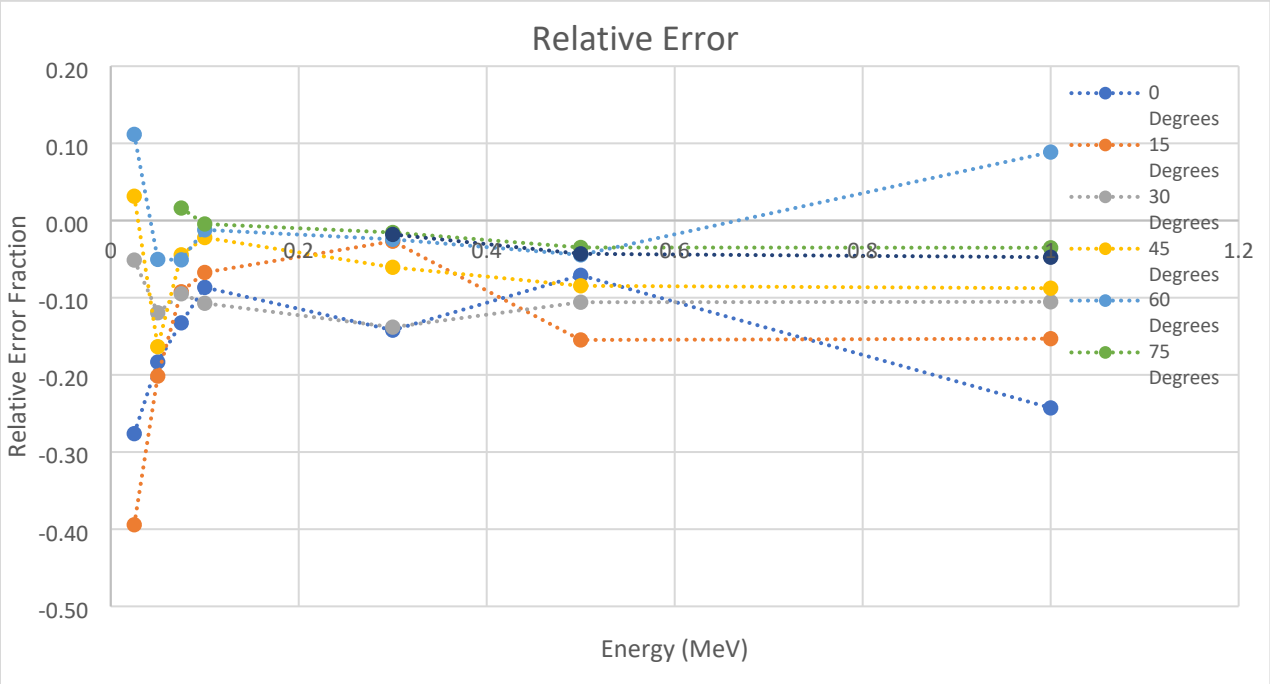

There is no way to give a test statistic to show how close we are necessarily with his data given his experimental errors.

Molybdenum

Molybdenum's ITS data against Lockwood's experimental data demonstrate good agreement in this material at all angles and energies, particularly at the higher energies. The experimental error in Lockwood's data was quite small. When looking at figure 9, it is clear that the ITS simulation albedos and those of Lockwood's don't exactly sit on top of each other for the lower energies, but when looking at how "close" they are to each other, figure 10 demonstrates that the relative error at the lower energies is at or less than five percent.

FIG. 9. Incident Energy v. Fraction of Electrons Backscattered for Molybdenum

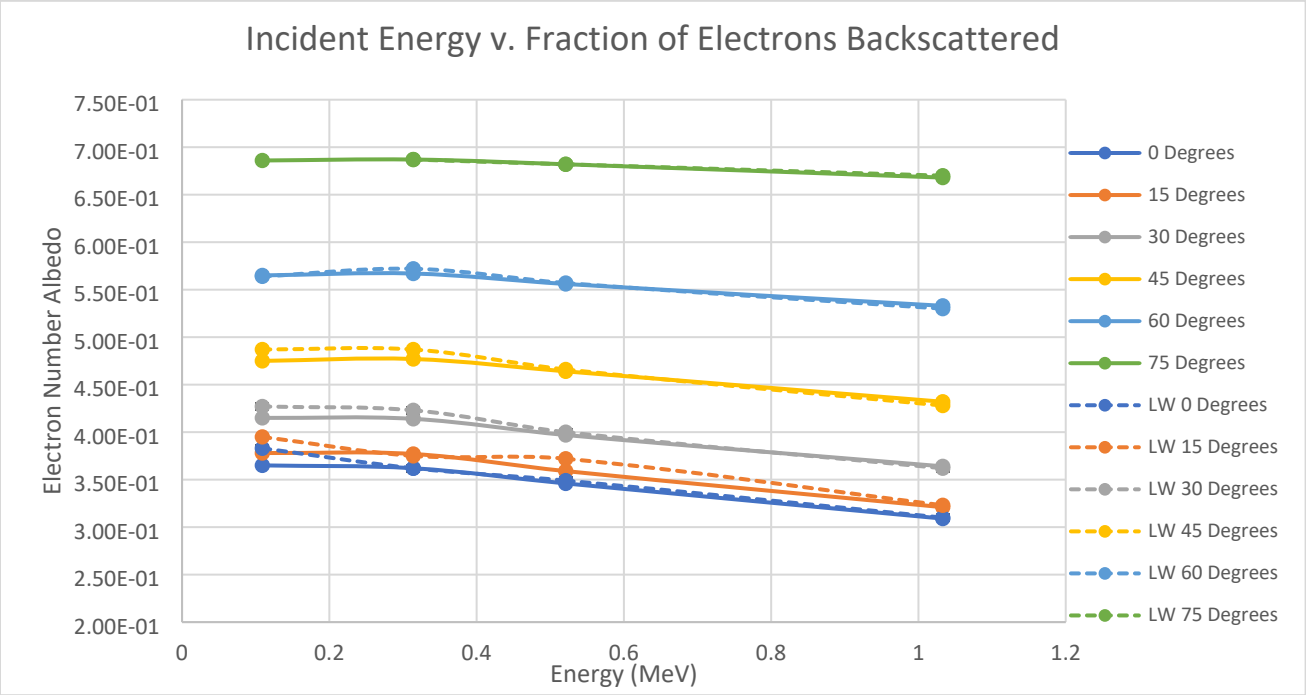

When looking at relative error, the highest point seen is at about 5 percent relative error, with all angles converging down to at or under 1 percent. This trend would point to there being good agreement throughout the data, with there being stronger agreement as incident energy levels increase.

FIG. 10. Relative Error for Molybdenum

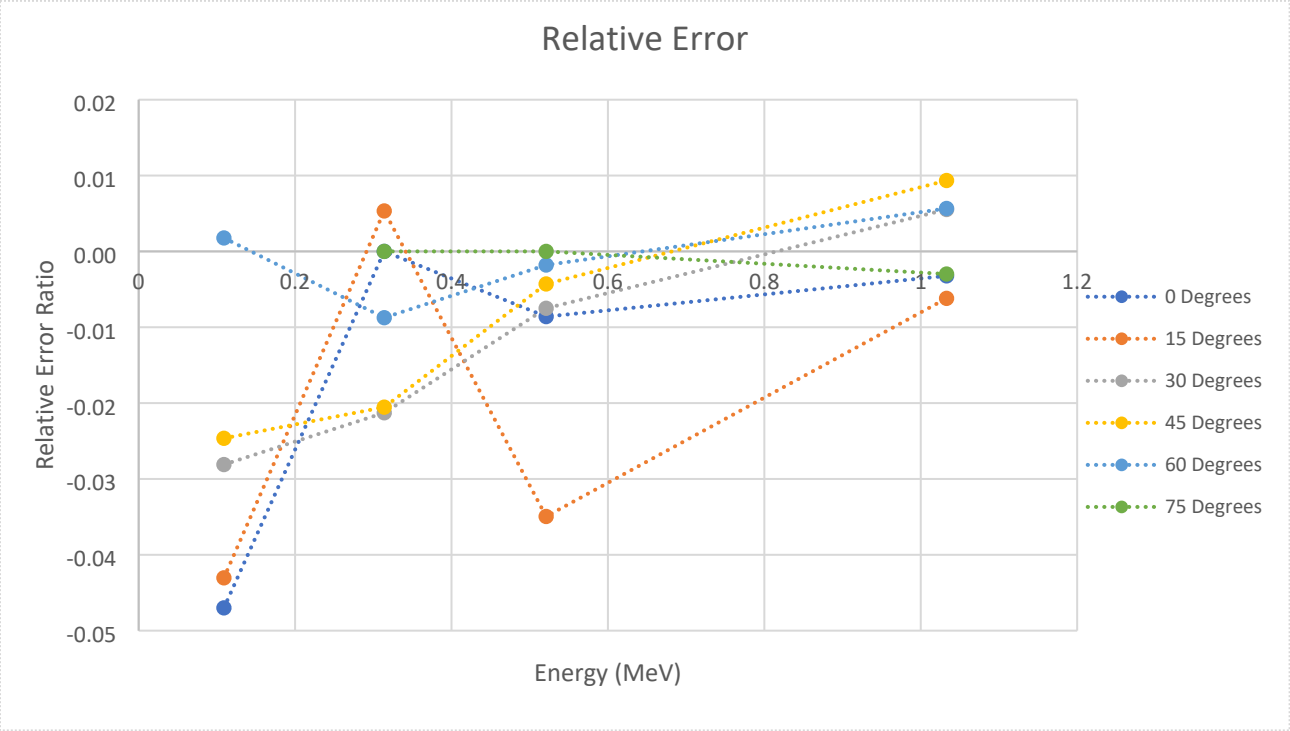

With respect to the overall test statistics, the lower angles show a strong relationship that is around 0.1 to about 0.12. A point is missing from 75 degrees at 0.109 MeV due to there not being a point of comparison to Lockwood's data. The lower angles at lower energies express the highest percentage of relative error. The general trend overall for the test statistical error is that as energy increases, the error decreases.

FIG. 11. Error relative to the combined statistical error for Molybdenum

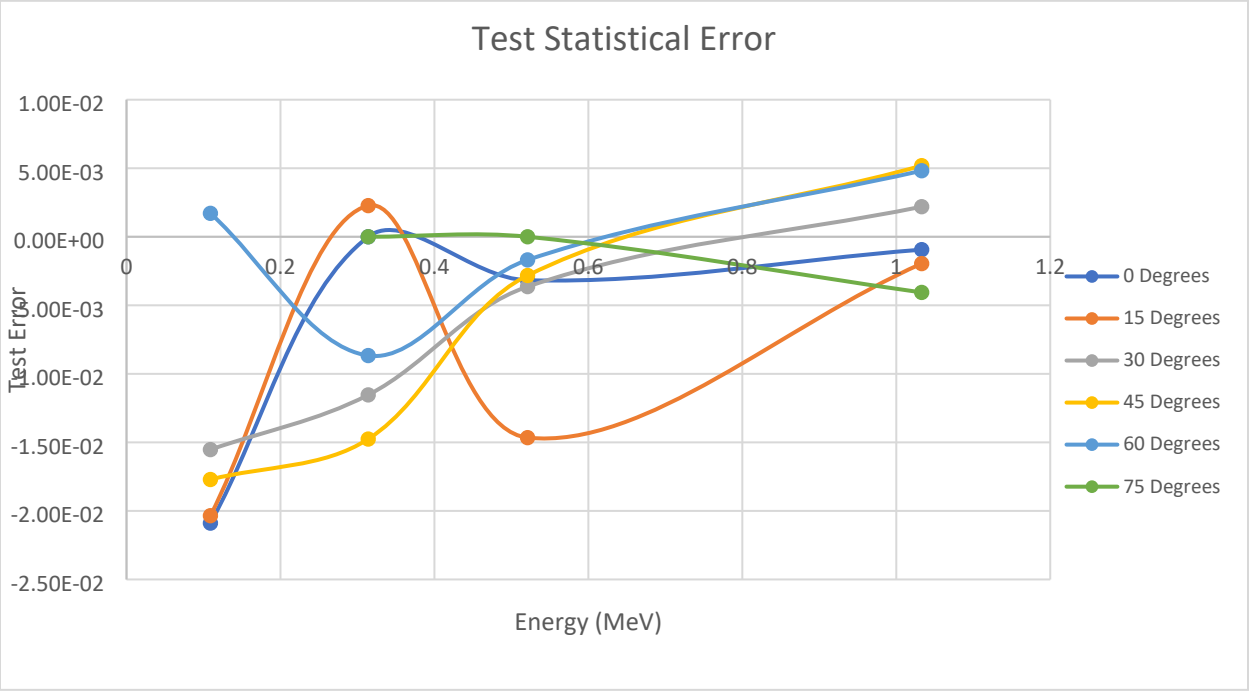

Titanium

When looking comparatively between the ITS Simulation data and Lockwood's albedo data, there appears to be strong agreement between the two data sets, with minimal error on both sets of data. As energy increases, it appears that the albedo decreases, as does the error in the data sets. The closest agreement happens in the mid-ranged energies of 0.314 MeV and 0.521 MeV. The trend in a majority of the data is quite linear, showing a linear change in the electrons reflected as energy increases.

FIG. 12. Incident Electron Energy v. Fraction of Electrons Backscattered in Titanium

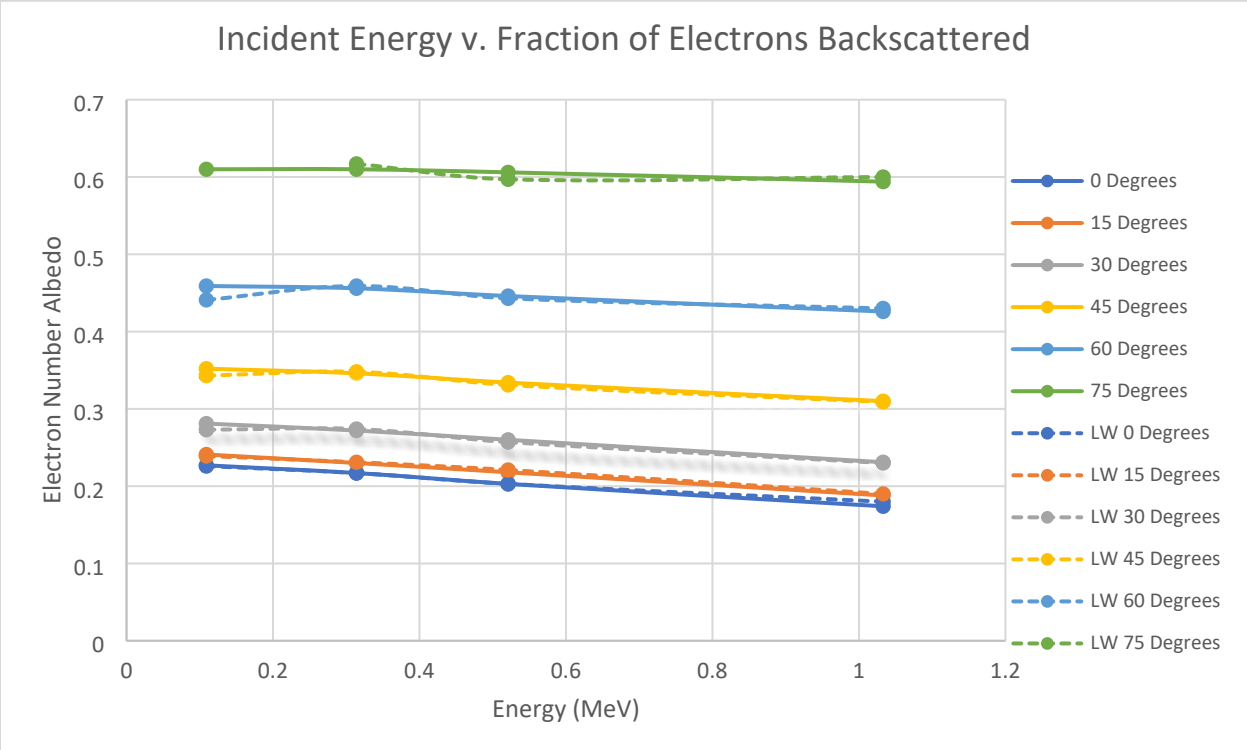

The relative error for Titanium is rather low, with the highest point peaking just above 4 percent. For all but 0 degrees, the relative error at 1.033 MeV is lower than (or the same as) it was at 0.109 MeV. The relative error for 0 degrees changed from just under 0.5 percent to almost 3.5 percent. This may be in part to Lockwood not having a data point present, which has the potential to increase the relative error. This trend in decreasing relative error supports the initial finding that there is better agreement for this data as energy increases, and furthermore that given the small magnitude of the relative error at even the highest points, that the results in the simulation data show strong agreement with that of Lockwood's data.

FIG. 13. Relative Error for Titanium

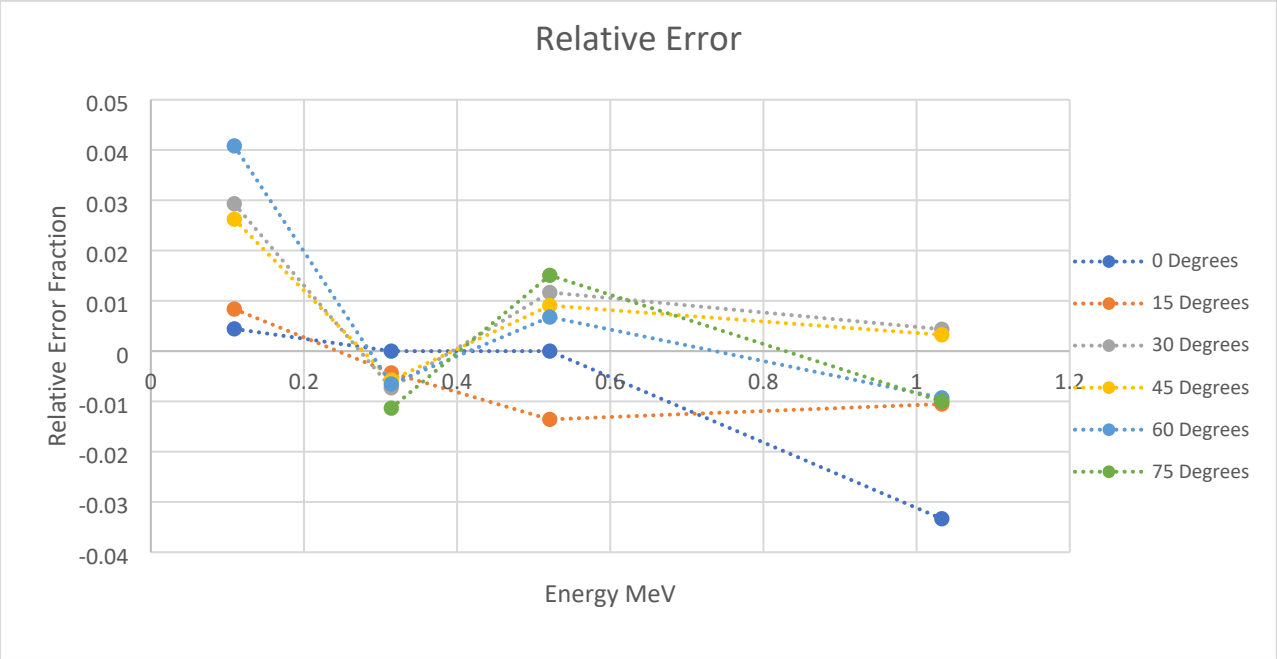

The combined statistical error for Titanium is generally low overall. There is no combined statistical error for 0.109 MeV at 75 degrees in part of Lockwood not having a data point to compare to. The highest combined error observed for Titanium occurs at 60 degrees and 0.109 MeV. The combined error values decrease as the energy increases, for all angels. This demonstrates once again that there is a strong agreement between the simulation data and Lockwood's data, and that the agreement is stronger still at higher energies.

FIG. 14. Error relative to the combined statistical error for Titanium

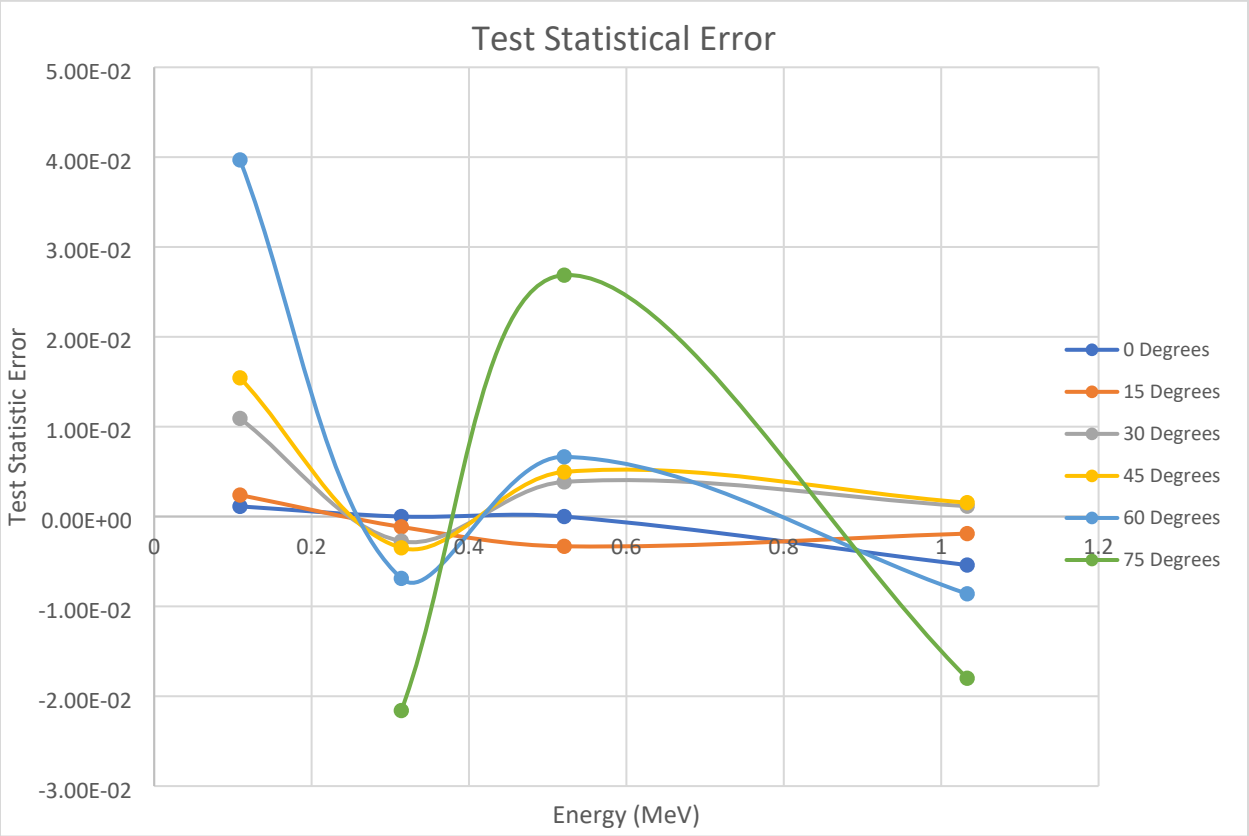

Tantalum

Tantalum shows little agreement in the lower energies, especially at 60 degrees and at 0.032 MeV. Error in this data is highest at 0 degrees and at 0.032 MeV. The albedos peak at around 0.314 MeV, and then decrease, for both in simulation and Lockwood data. As the energy increases, the albedo decreases. There is also stronger agreement in the higher energies, particularly after 0.314 MeV.

FIG. 15. Incident Energy v. Fraction of Electrons Backscattered for Tantalum

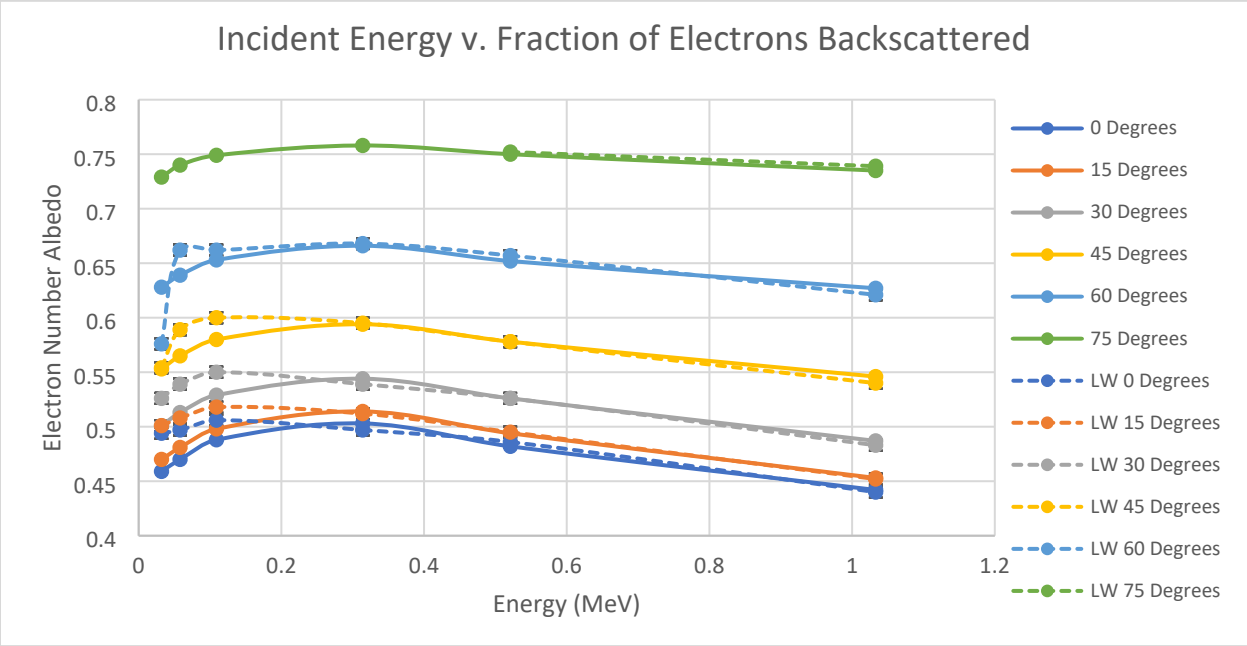

The peak relative error in this data set is around 9 percent, which occurs at 60 degrees and at 0.032 MeV, as figure 15 would also suggest. Most angles in this data set have initially high relative error at 0.032 MeV, respectively, with the exception of 45 degrees at less than 1 percent. As energy increases, relative error does as well, dropping below 2 percent for all angles. This shows that there is strong agreement for Tantalum in the higher energies.

FIG. 16 Relative Error for Tantalum

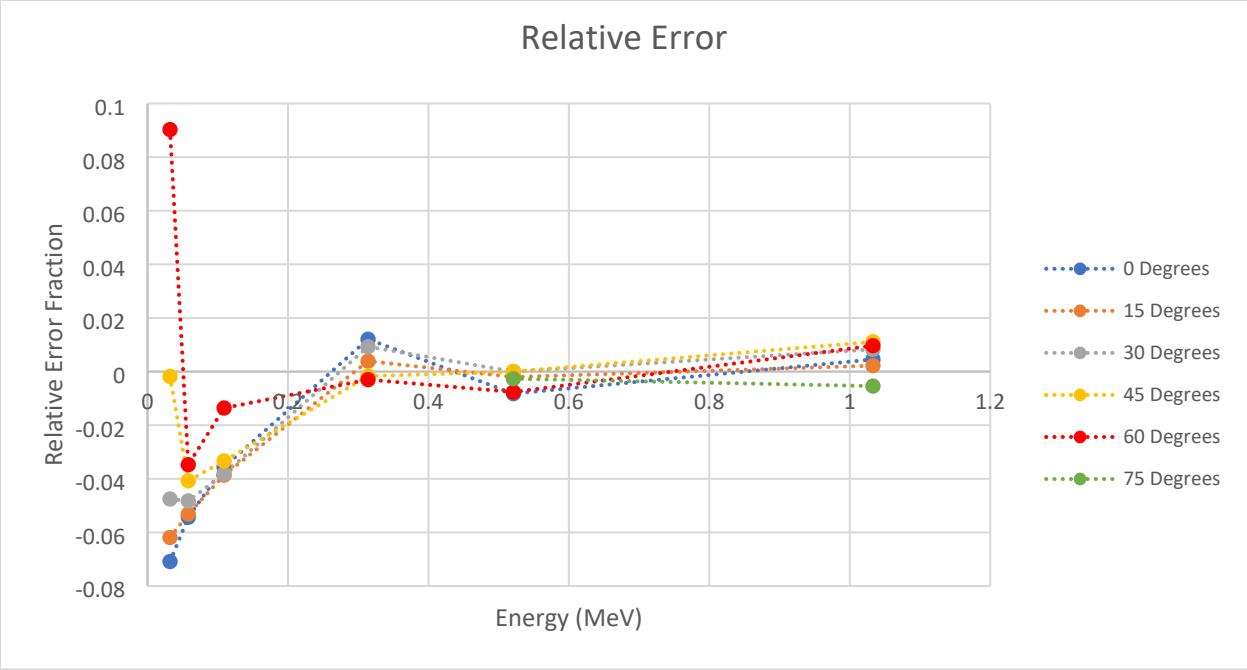

When looking at the overall test statistical error, 4 points were omitted from the figure 17, as their test statistical error was much higher than any other point (which can be seen in the appendix). Apart from that, the highest error is just under 4 percent, and the test statistic improves as energy increases, with all angles coming just under 0.5 percent. This shows stronger agreement at higher energies as opposed to the lower energies.

FIG. 17. Error relative to the combined statistical error for Tantalum

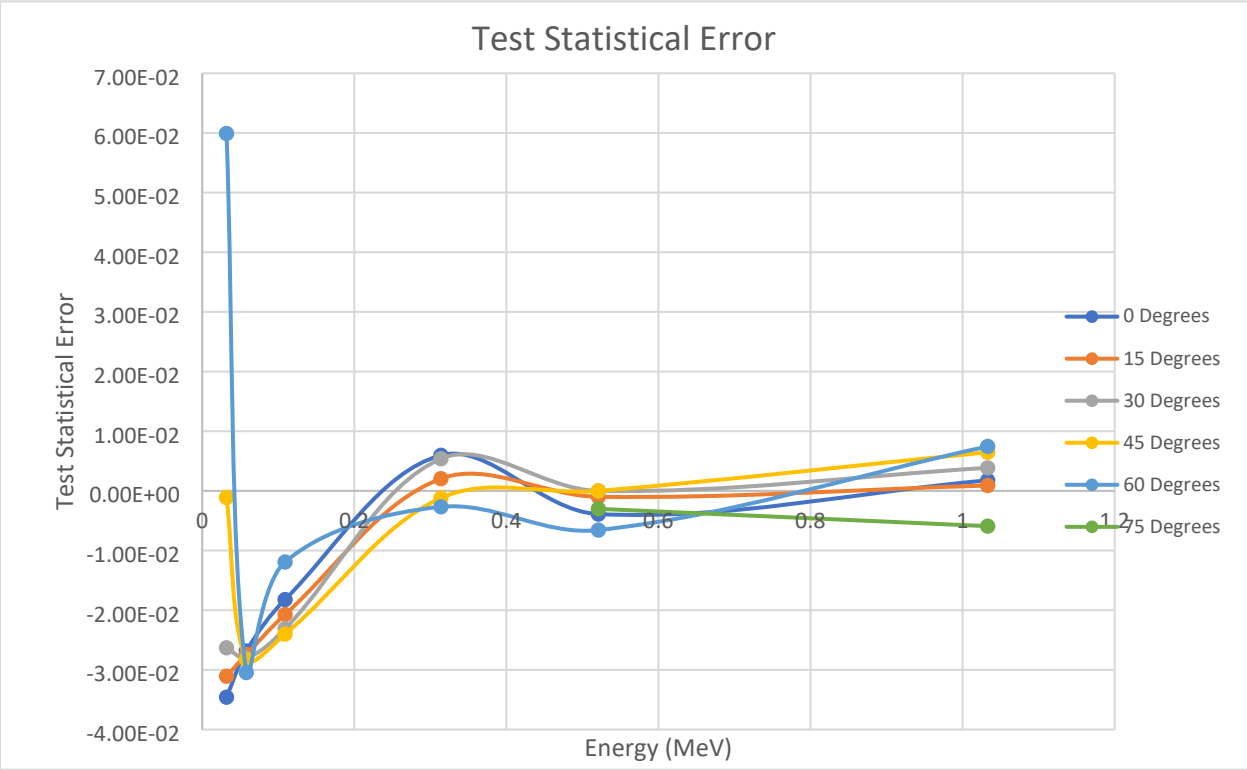

Uranium

Uranium does not show great agreement in the lower energies, particularly at 0.032 MeV in the 60 degree and 45 degree angles. In particular, the albedo numbers form the ITS Simulation are higher than those reported by Lockwood's experiment throughout the results for Uranium. Agreement is stronger in the higher angles. There is also no point of reference for Lockwood's data for 75 degrees and 0.032 or 0.058 MeV. This ultimately may lead to a source of error when looking at how close the ITS simulation is to Lockwood's data, particularly at lower energies.

FIG. 18. Incident Energy v. Fraction of Electrons Backscattered for Uranium

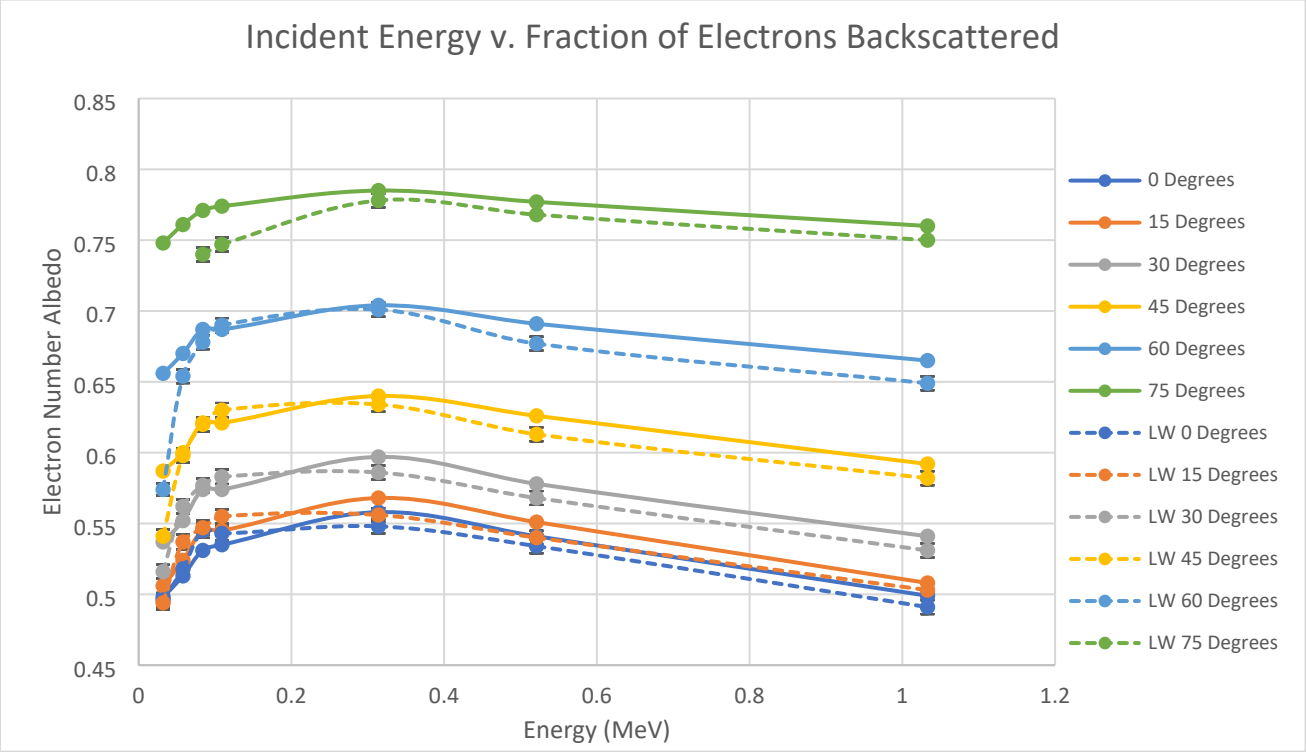

As shown in the data above in figure 18, the potential disagreement in the number albedos is also reflected in the relative error between the Lockwood and Simulation data. The relative error is greatest for 60 degrees at 0.032 MeV, and all relative error eventually comes down to about 2 percent at 1.033 MeV, demonstrating good agreement in the simulation values with those of Lockwood's in higher energies. With the exception of 0 degrees, whose error is lowest at 0.032 MeV, the relative error for all angles decreases as energy increases.

FIG. 19. Relative Error for Uranium

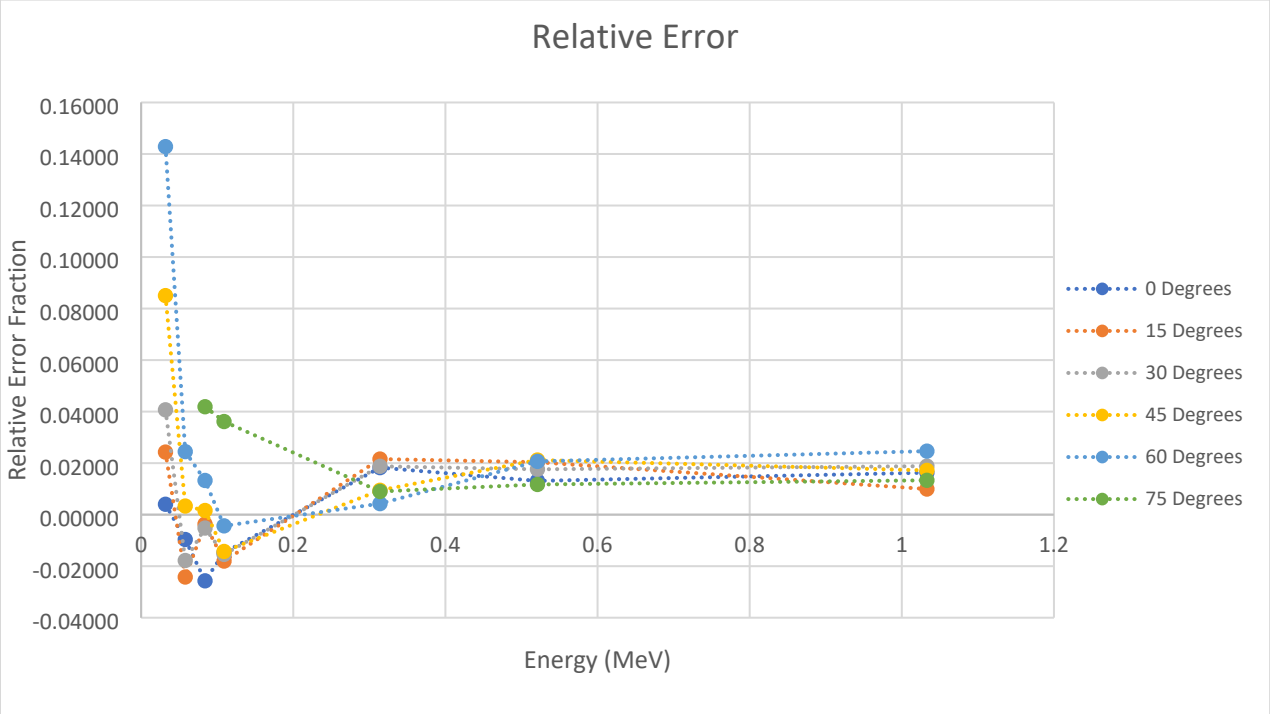

In looking at the overall test statistic, two points are removed graphically for 75 degrees at 0.032 and 0.058 MeV due to their high percent. Their high percent is most likely due to Lockwood not having an experimental error datapoint available for these energies. Apart from that, the next highest point is for 65 degrees at about 6 percent, which then decreases to just over 1 percent error. The lowest error value is seen for 15 degrees, which is almost 0 percent, at 1.033 MeV.

FIG. 20. Error relative to the combined statistical error for Uranium

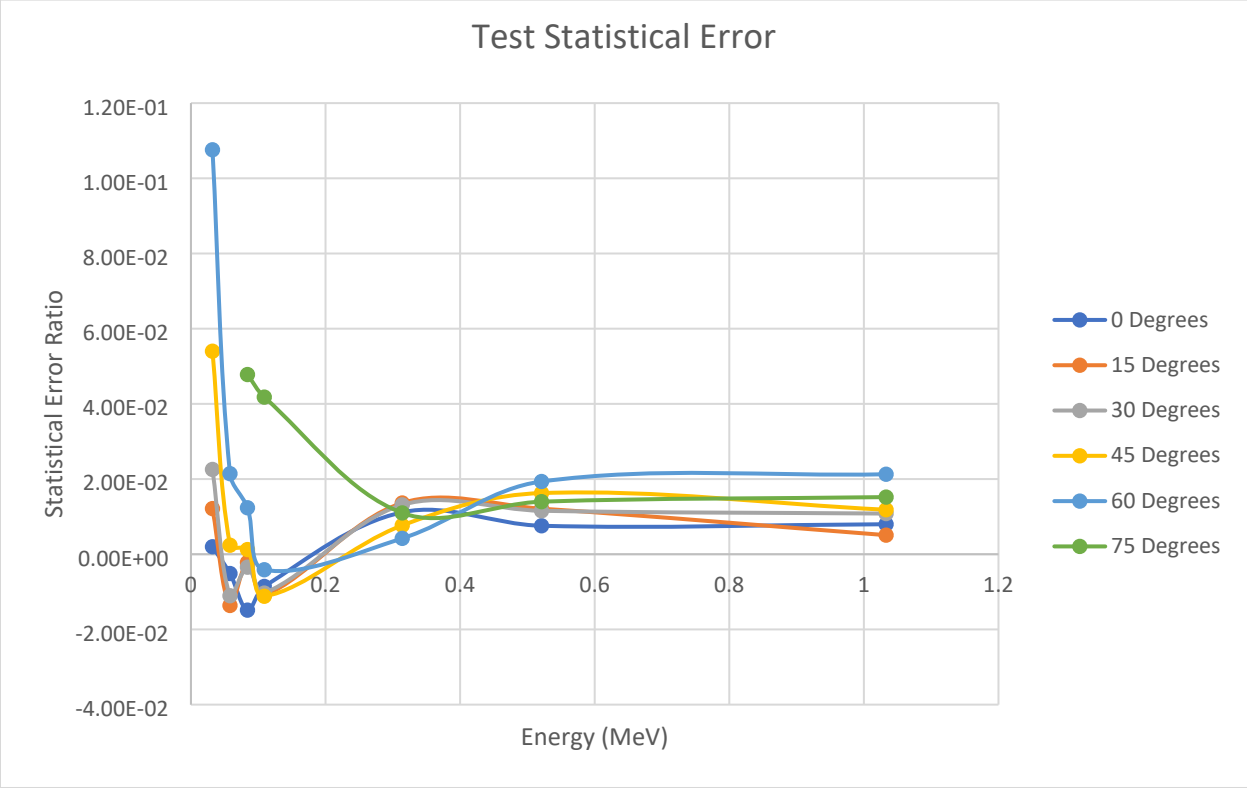

Uranium Dioxide

Uranium Dioxide, or Urania, shows good agreement in the low angles at all energies, but as the angles increase, the agreement becomes worse at 0.1 MeV. However, the higher angles start to show stronger agreement as energy increases, especially at 75 degrees. The reported albedos for the simulation are highest around 0.3 MeV, and then the lowest at 1 MeV. Lockwood did not report any experimental error for Urania, and the simulation error was reported near 0.

FIG. 21. Incident Energy v. Fraction of Electrons Backscattered for Uranium Dioxide

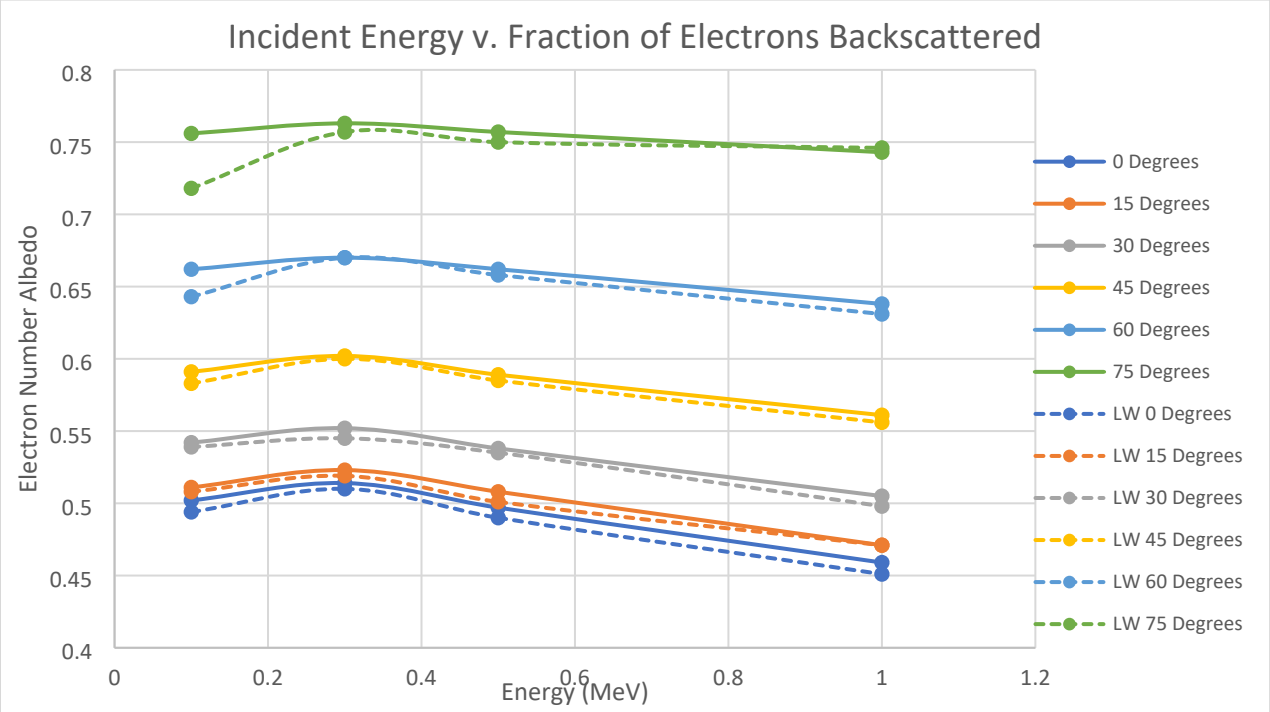

The relative error is less than 6 percent at its highest point. That highest point occurs at 75 degrees and 0.1 MeV. All error decreases for each angle as energy increases, with the exception of 0 degrees and 30 degrees, which increases slightly. 15 degrees shows error that trends to almost 0 at 1 MeV. This demonstrates that at higher energies, there is strong agreement, however in the case of Urania, there is relatively strong agreement throughout at all angles and energies.

FIG. 22. Relative Error for Uranium Dioxide

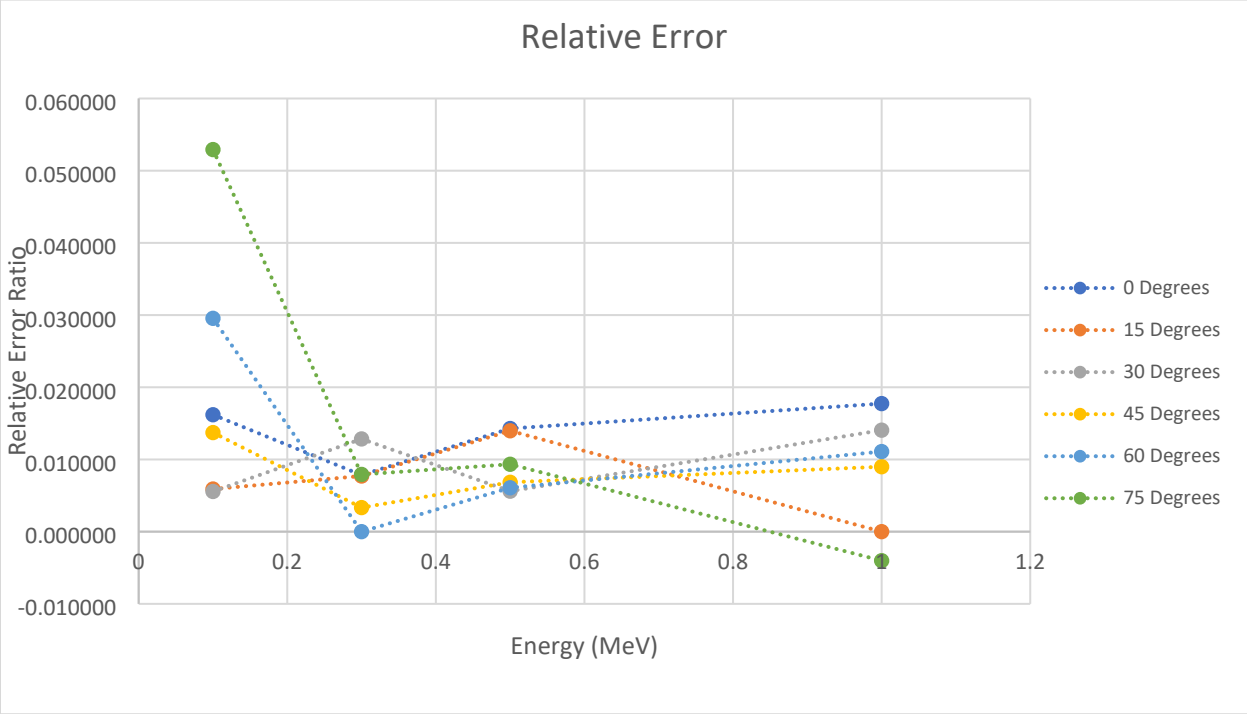

Conclusion

The ITS Simulation data overall shows good agreement for all materials at high energies, for all angles, and all Z values. The error is low at the endpoint energies of each simulation, both relatively and for the test itself. However, on the lower band of energies, especially in the high angles (75/76 degrees or 82.5/83.5) there is poor agreement. This is exacerbated even more so in the lower Z materials tested, such as Aluminum, Carbon, and Beryllium. As Z increase, agreement in these values, while still not great, improves. The general test statistical error values are low, at least for those values in which Lockwood provided a quantitative error value that which a comparison might be made to with the ITS Simulation data. This shows that baring the aforementioned issues, the ITS code does have strong and reliable physical models that simulate (within at most a 10 percent error) accurate results.

Despite the results being relatively accurate, it is clear that there is room for potential improvement of the physical models for lower Z materials, and potentially lower energies. Although it may simply be enough to let users know a band of uncertainty that their results may fall within. However, for that to be achievable and realistic, more data sets will need to be run with increased histories and histories per batch to increase test accuracy further in the simulations. It may also be relevant for future tests to look at more statistical analysis for a stronger understanding on the accuracy of the low z, low energy results.

Acknowledgements

Supported by the Laboratory Directed Research and Development program at Sandia National Laboratories, a multimission laboratory managed and operated by National Technology and Engineering Solutions of Sandia LLC, a wholly owned subsidiary of Honeywell International Inc. for the U.S. Department of Energy's National Nuclear Security Administration under contract DE-NA0003525.

This paper describes objective technical results and analysis. Any subjective views or opinions that might be expressed in the paper do not necessarily represent the views of the U.S. Department of Energy or the United States Government.

The results of this paper were ultimately made possible with the assistance, guidance, and education from all names listed on the front of this paper, as well as Dr. Daryl Lee of the University of New Mexico's COSMIAC Research Institute. His assistance in teaching me coding techniques in Python and Shell have allowed me to complete the necessary tasks in a reasonable time, in an effective and accurate way.

Appendix

A. Beryllium Relative Error

Energy / Angle	1	16	31	46	61	76	83.5
0.109 MeV	-0.13	-0.10	0.10	0.05			
0.314 MeV	-0.24	-0.21	-0.07	0.03	0.07	0.07	
0.521 MeV	-0.36	-0.17	-0.06	0.04	0.05	0.07	0.04
1.033 MeV	-0.26	-0.27	-0.11	0.02	0.05	0.03	0.02

B. Aluminum Relative Error

Energy / Angle	0	15	30	45	60	75
0.032 MeV	0	-6.33E-02	1.63E-01	4.33E-01	5.89E-01	6.17E-01
0.058 MeV	-6.43E-02	-6.54E-02	-4.23E-02	2.83E-02	8.53E-02	0.00E+00
0.084 MeV	-5.00E-02	-3.97E-02	0.00E+00	7.08E-02	1.36E-02	-2.33E-02
0.109 MeV	-3.68E-02	-7.79E-02	0.00E+00	-1.17E-02	1.92E-02	-1.97E-02
0.314 MeV	1.64E-02	-1.45E-02	5.68E-03	-3.97E-03	1.93E-02	-7.26E-03
0.521 MeV	2.70E-02	8.00E-03	3.09E-02	4.29E-02	2.54E-02	2.06E-02
1.033 MeV	-8.70E-03	-9.62E-03	4.35E-02	2.80E-02	2.08E-02	1.13E-02

C. Carbon Relative Error

Energy / Angle	0	15	30	45	60	75	82.5
0.025 MeV	-0.28	-0.39	-0.05	0.03	0.11		
0.05 MeV	-0.18	-0.20	-0.12	-0.16	-0.05		
0.075 MeV	-0.13	-0.09	-0.09	-0.04	-0.05	0.02	
0.1 MeV	-0.09	-0.07	-0.11	-0.02	-0.01	0.00	
0.3 MeV	-0.14	-0.03	-0.14	-0.06	-0.02	-0.02	-0.02
0.5 MeV	-0.07	-0.15	-0.11	-0.08	-0.04	-0.03	-0.04
1 MeV	-0.24	-0.15	-0.11	-0.09	0.09	-0.04	-0.05

D. Molybdenum Relative Error

Energy / Angle	0	15	30	45	60	75
0.109 MeV	-0.05	-0.04	-0.03	-0.02	0.00	
0.314 MeV	0.00	0.01	-0.02	-0.02	-0.01	0.00
0.521 MeV	-0.01	-0.03	-0.01	0.00	0.00	0.00
1.033 MeV	0.00	-0.01	0.01	0.01	0.01	0.00

E. Titanium Relative Error

Energy / Angle	0	15	30	45	60	75
0.109 MeV	0.0044248	0.0083682	0.02930403	0.02623907	0.04081633	
0.314 MeV	0	-0.004329	-0.0072993	-0.0057471	-0.0065359	-0.011345
0.521 MeV	0	-0.013575	0.01167315	0.00906344	0.00677201	0.0150754
1.033 MeV	-0.0333333	-0.010526	0.00434783	0.00323625	-0.0093023	-0.01

F. Tantalum Relative Error

Energy / Angle	0	15	30	45	60	75
0.032 MeV	-0.07085	-0.061876	-0.047529	-0.0018051	0.0902778	
0.058 MeV	-0.05433	-0.05315	-0.048238	-0.040747	-0.034743	
0.109 MeV	-0.035573	-0.03861	-0.038182	-0.0333333	-0.013595	
0.314 MeV	0.0120724	0.0039063	0.0092764	-0.0016807	-0.002994	
0.521 MeV	-0.008231	-0.0020202	0	0	-0.00761	-0.00266
1.033 MeV	0.0045455	0.0022124	0.0082816	0.0111111	0.009662	-0.005413

G. Uranium Relative Error

Energy / Angle	0	15	30	45	60	75
0.032 MeV	0.00403	0.02429	0.04070	0.08503	0.14286	
0.058 MeV	-0.00965	-0.02421	-0.01779	0.00334	0.02446	
0.084 MeV	-0.02569	-0.00366	-0.00520	0.00161	0.01327	0.04189
0.109 MeV	-0.01473	-0.01802	-0.01544	-0.01429	-0.00435	0.03614
0.314 MeV	0.01825	0.02158	0.01877	0.00946	0.00428	0.00900
0.521 MeV	0.01311	0.02037	0.01761	0.02121	0.02068	0.01172
1.033 MeV	0.01629	0.00994	0.01883	0.01718	0.02465	0.01333

H. Uranium Dioxide Relative Error

Energy / Angle	0	15	30	45	60	75
0.1 MeV	0.016194	0.005906	0.005566	0.013722	0.029549	0.052925
0.3 MeV	0.007843	0.007707	0.012844	0.003333	0.000000	0.007926
0.5 MeV	0.014286	0.013972	0.005607	0.006838	0.006079	0.009333
1 MeV	0.017738	0.000000	0.014056	0.008993	0.011094	-0.004021

I. Simulation Error for Beryllium

Energy / Angle	1	16	31	46	61	76	83.5
0.109 MeV	2.93E-04	3.63E-04	6.29E-04	4.43E-04	9.85E-04	2.05E-03	2.91E-03
0.314 MeV	2.40E-04	3.12E-04	5.75E-04	4.29E-04	9.80E-04	2.08E-03	2.95E-03
0.521 MeV	2.03E-04	2.72E-04	5.28E-04	4.12E-04	9.60E-04	2.07E-03	2.97E-03
1.033 MeV	1.34E-04	1.91E-04	4.10E-04	3.54E-04	8.95E-04	2.04E-03	2.97E-03

J. Simulation Error for Aluminum

Energy / Angle	0	15	30	45	60	75
0.032 MeV	6.85E-04	7.40E-04	9.30E-04	1.28E-03	1.84E-03	2.69E-03
0.058 MeV	6.55E-04	7.15E-04	9.05E-04	1.27E-03	1.85E-03	2.71E-03
0.084 MeV	6.65E-04	7.25E-04	9.20E-04	1.29E-03	1.87E-03	2.73E-03
0.109 MeV	6.55E-04	7.10E-04	9.05E-04	1.27E-03	1.86E-03	2.74E-03
0.314 MeV	6.20E-04	6.80E-04	8.85E-04	1.26E-03	1.85E-03	2.74E-03
0.521 MeV	5.70E-04	6.30E-04	8.35E-04	1.22E-03	1.82E-03	2.72E-03
1.033 MeV	4.56E-04	5.15E-04	7.20E-04	1.10E-03	1.72E-03	2.69E-03

K. Simulation Error for Molybdenum

Energy / Angle	0	15	30	45	60	75
0.109 MeV	1.83E-03	1.89E-03	2.08E-03	2.38E-03	2.83E-03	
0.314 MeV	1.81E-03	1.89E-03	2.07E-03	2.39E-03	2.84E-03	3.44E-03
0.521 MeV	1.73E-03	1.80E-03	1.99E-03	2.32E-03	2.78E-03	3.41E-03
1.033 MeV	1.55E-03	1.61E-03	1.82E-03	2.16E-03	2.67E-03	3.34E-03

L. Simulation Error for Titanium

Energy / Angle	0	15	30	45	60	75
0.109 MeV	0.001135	0.001205	0.001405	0.00176	0.002295	0.00305
0.314 MeV	0.001085	0.00115	0.00136	0.00173	0.00228	0.00305
0.521 MeV	0.001015	0.00109	0.0013	0.00167	0.00223	0.00303
1.033 MeV	0.00087	0.00094	0.001155	0.00155	0.00213	0.00297

M. Simulation Error for Tantalum

Energy / Angle	0	15	30	45	60	75
0.032 MeV	0.002295	0.00235	0.002505	0.002765	0.00314	
0.058 MeV	0.00235	0.002405	0.002565	0.002825	0.003195	
0.109 MeV	0.00244	0.00249	0.002645	0.0029	0.003265	
0.314 MeV	0.002515	0.00257	0.00272	0.00297	0.00333	
0.521 MeV	0.00241	0.00247	0.00263	0.00289	0.00326	0.00375
1.033 MeV	0.00221	0.002265	0.002435	0.00273	0.003135	0.003675

N. Simulation Error for Uranium

Energy / Angle	0	15	30	45	60	75
0.032 MeV	0.00249	0.00253	0.002685	0.002935	0.00328	0.00374
0.058 MeV	0.002565	0.00262	0.00276	0.003	0.00335	0.003805
0.084 MeV	0.002655	0.002725	0.00287	0.003105	0.003435	0.003855
0.109 MeV	0.002675	0.002725	0.00287	0.003105	0.003435	0.00387
0.314 MeV	0.00279	0.00284	0.002985	0.0032	0.00352	0.003925
0.521 MeV	0.002705	0.002755	0.00289	0.00313	0.003455	0.003885
1.033 MeV	0.002495	0.00254	0.002705	0.00296	0.003325	0.0038

O. Combined Statistical Error Values for Beryllium

Energy/ Angle	1	16	31	46	61	76	83.5
0.109 MeV	-2.08E-04	-2.32E-04	4.94E-04	1.29E-03	**200**	**200**	**200**
0.314 MeV	-3.50E-04	-4.82E-04	-3.69E-04	6.94E-04	7.36E-03	3.61E-02	**200**
0.521 MeV	-5.35E-04	-2.60E-04	-2.87E-04	8.94E-04	5.49E-03	3.48E-02	4.00E-02
1.033 MeV	-1.23E-04	-2.73E-04	-3.37E-04	2.55E-04	5.10E-03	1.58E-02	1.75E-02

P. Combined Statistical Error Values for Aluminum

Energy / Angle	0	15	30	45	60	75
0.032 MeV	0	-3.43E-03	9.04E-03	2.98E-02	6.83E-02	1.48E-01
0.058 MeV	-2.74E-03	-3.33E-03	-3.29E-03	3.76E-03	2.14E-02	0.00E+00
0.084 MeV	-2.13E-03	-1.97E-03	0.00E+00	8.87E-03	4.00E-03	-1.58E-02
0.109 MeV	-1.48E-03	-4.02E-03	0.00E+00	-1.68E-03	5.55E-03	-1.33E-02
0.314 MeV	5.30E-04	-6.00E-04	3.83E-04	-5.48E-04	5.52E-03	-4.79E-03
0.521 MeV	7.24E-04	2.72E-04	1.76E-03	5.07E-03	6.93E-03	1.27E-02
1.033 MeV	-1.60E-04	-2.26E-04	1.80E-03	2.79E-03	5.13E-03	6.93E-03

Q. Combined Statistical Error Values for Molybdenum

Energy / Angle	0	15	30	45	60	75
0.109 MeV	-2.09E-02	-2.03E-02	-1.55E-02	-1.77E-02	1.71E-03	
0.314 MeV	0.00E+00	2.27E-03	-1.15E-02	-1.48E-02	-8.67E-03	0.00E+00
0.521 MeV	-3.17E-03	-1.47E-02	-3.64E-03	-2.82E-03	-1.69E-03	0.00E+00
1.033 MeV	-9.39E-04	-1.96E-03	2.19E-03	5.19E-03	4.82E-03	-4.06E-03

R. Combined Statistical Error Values for Titanium

Energy / Angle	0	15	30	45	60	75
0.109 MeV	1.13E-03	2.39E-03	1.09E-02	1.54E-02	3.97E-02	**2.00E+02**
0.314 MeV	0.00E+00	-1.15E-03	-2.74E-03	-3.48E-03	-6.88E-03	-2.16E-02
0.521 MeV	0.00E+00	-3.31E-03	3.85E-03	4.96E-03	6.64E-03	2.69E-02
1.033 MeV	-5.40E-03	-1.90E-03	1.15E-03	1.54E-03	-8.60E-03	-1.80E-02

S. Combined Statistical Error Values for Tantalum

Energy / Angle	0	15	30	45	60	75
0.032 MeV	-3.46E-02	-3.11E-02	-2.63E-02	-1.11E-03	5.99E-02	
0.058 MeV	-2.68E-02	-2.74E-02	-2.80E-02	-2.83E-02	-3.05E-02	
0.109 MeV	-1.82E-02	-2.07E-02	-2.31E-02	-2.40E-02	-1.19E-02	
0.314 MeV	5.96E-03	2.05E-03	5.39E-03	-1.19E-03	-2.67E-03	
0.521 MeV	-3.89E-03	-9.90E-04	0.00E+00	0.00E+00	-6.57E-03	-3.01E-03
1.033 MeV	1.76E-03	9.04E-04	3.86E-03	6.48E-03	7.45E-03	-5.91E-03

T. Combined Statistical Error Values for Uranium

Energy / Angle	0	15	30	45	60	75
0.032 MeV	1.99E-03	1.21E-02	2.26E-02	5.40E-02	1.08E-01	
0.058 MeV	-5.13E-03	-1.36E-02	-1.10E-02	2.40E-03	2.14E-02	
0.084 MeV	-1.49E-02	-2.18E-03	-3.44E-03	1.24E-03	1.24E-02	4.78E-02
0.109 MeV	-8.56E-03	-1.09E-02	-1.03E-02	-1.12E-02	-4.12E-03	4.18E-02
0.314 MeV	1.12E-02	1.36E-02	1.31E-02	7.68E-03	4.22E-03	1.10E-02
0.521 MeV	7.57E-03	1.21E-02	1.16E-02	1.63E-02	1.93E-02	1.40E-02
1.033 MeV	7.98E-03	5.08E-03	1.08E-02	1.18E-02	2.13E-02	1.52E-02

U. “C” Values (From Eq. 3)

	Be	Al	C	Mo	Ti	Ta	U	UO2
C Value	0.30	0.46	N/A	0.33	0.20	0.50	0.50	N/A

References

1. B. C. FRANKE, R. P. KENSEK, "Electron Transport Algorithms in the Integrated Tiger Series (ITS) Codes," American Nuclear Society RPSD (2018).
2. B. C. FRANKE, et al., "ITS Version 6: The Integrated TIGER Series of Coupled Electron/Photon Monte Carlo Transport codes, Revision 5," SAND2008-3331, Sandia National Laboratories, PO Box 5800, Albuquerque, NM. 87185, September 2013.
3. G. J. LOCKWOOD, L. E. RUGGLES, G. H. MILLER, and J. A. HALBLEIB, "Electron energy and charge albedos calorimetric measurement vs Monte Carlo theory," Tech. Rep. SAND80-1968, Sandia National Laboratories (1981).
4. A. O. HANSON, L. H. LANZL, E. M. LYMAN, and M. B. SCOTT, "Measurement of Multiple Scattering of 15.7 MeV Electrons," *Physical Review*, **84**, *4* (1951).
5. T. TABATA, R. ITO, and S. OKABE, "Charge Distribution Produced by 4 to 24 MeV Electrons in Elemental Materials," *Physical Review B,* **3**, *3* (1971).
6. W. L. MCLAUGHLIN and E. K. HUSSMAN, "The Measurement of Electron and Gamma-Ray Dose Distributions in Various Media," in "Large Radiation Sources for Industrial Processes," IAEA-SM-123/43.
7. J. A. HALBLEIB, T. W. L. SANFORD, and W. BEEZHOLD, "Experimental Verification of Bremsstrahlung Dosimetry Predictions for 0.75 MeV Electrons, "Tech. Rep. SAND85-1517," Sandia National Laboratories (1986).
8. K. W. DOLAN, "X-ray-Induced Electron Emission from Metals," *J. Appl. Phys.,* **46**, *6,* 2456-2463 (1975).
9. M. J. BERGER, "Monte Carlo Calculations of the Penetration and Diffusion of Fast Charged Particles," in B. ALDER, S. FERNBACH, and M. ROTENBERG, editors, "Methods in Computational Physics, Vol. 1," Academic Press, New York (1963).
10. S. M. SELTZER, "An overview of ETRAN Monte Carlo methods," in T. M. JENKINS, W. R. NELSON, and A. RINDI, editors, "Monte Carlo Transport of electrons and photons," Plenum Press, New York, Ettore Majorana International Science Series: Physical Sciences (1988).
11. J. A. HALBLEIB and J. E. MOREL, "Adjoint Monte Carlo electron transport in the continuous slowing-down approximation," *J. Comp. Phys.,* **34**, 211 (1980).
12. G. J. LOCKWOOD, G. H. MILLER, and J. A. HALBLEIB, "Simultaneous Integral Measurement of Electron Energy and Charge Albedos," *IEEE Transactions on Nuclear Science,* **NS-22**, *6* (1975).
13. G. J. LOCKWOOD, J. A. HALBLEIB, G. H. MILLER, "Electron Transport in Reactor Materials," *IEEE Transactions of Nuclear Science,* **NS-25**, *6*, (1978).

APPENDIX B.

DISTRIBUTION

Email—Internal

Name	Org.	Sandia Email Address
Aaron Olson	01341	Aolson@sandia.gov
Joseph P. Castro	01341	jpcastr@sandia.gov
Technical Library	01977	sanddocs@sandia.gov

Email—External (encrypt for OUO)

Name	Company Email Address	Company Name

Hardcopy—Internal

Number of Copies	Name	Org.	Mailstop

Hardcopy—External

Number of Copies	Name	Company Name and Company Mailing Address

This page left blank

This page left blank

Sandia National Laboratories

Sandia National Laboratories is a multimission laboratory managed and operated by National Technology & Engineering Solutions of Sandia LLC, a wholly owned subsidiary of Honeywell International Inc. for the U.S. Department of Energy's National Nuclear Security Administration under contract DE-NA0003525.